Cover Page

Project Title:	Membrane Carbonation for 100% Efficient Delivery of Industrial CO_2 Gases
Project Period:	Jan 1, 2019 – June 30, 2022
Reporting Period:	Jan 1, 2019 – September 30, 2022
Reporting Frequency:	Final
Recipient:	Arizona State University
Website:	www.asu.edu
Award Number:	DE-EE0008517
Awarding Agency:	DOE EERE – Bioenergy Technology Office: Efficient Carbon Utilization in Algal Systems (ECUAS)
Working Partners:	Sustainability Science, LLC; City of Mesa Arizona
Cost-Sharing Partners:	Sustainability Science, LLC; City of Mesa Arizona
Principal Investigator:	Dr. Bruce Rittmann Regents' Professor of Environmental Engineering Director of the Biodesign Swette Center for Environmental Biotechnology (480)727-0434 Rittmann@asu.edu
Submitted by:	Justin Flory
DOE Contracting Officer:	Andrew Rittgers
DOE Project Manager:	Christy Sterner

Disclaimer

Acknowledgment

This material is based upon work supported by the U.S. Department of Energy's Office of Energy Efficiency and Renewable Energy (EERE) under the Bioenergy Technologies Office, Award Number EE0008517.

Table of Contents

Executive Summary

Industrial processes generate about one quarter of all greenhouse gases emissions in the US, about 80% of which is carbon dioxide (CO_2). Biological processes are one of the largest natural sinks for atmospheric CO_2, but the rate of capture is limited by the low concentration in air (~0.04%). Industrial emissions have significantly higher CO_2 concentrations, ranging from 5–80% CO_2, which can significantly increase the rate of biological CO_2 capture, including many-fold improvements for cultivating microalgae to produce food, fertilizer, and renewable fuel. However, traditional methods for delivering CO_2 to microalgae using bubbling is < 40% efficient, leading to significant residual CO_2 emissions and increased cost. This project developed the Membrane Carbonation (MC) technology to significantly improve the CO_2 delivery efficiency to microalgae from power plant flue gas, wastewater treatment plant anaerobic digesters biogas (**Figure 1**), and other CO_2-containing industrial sources.

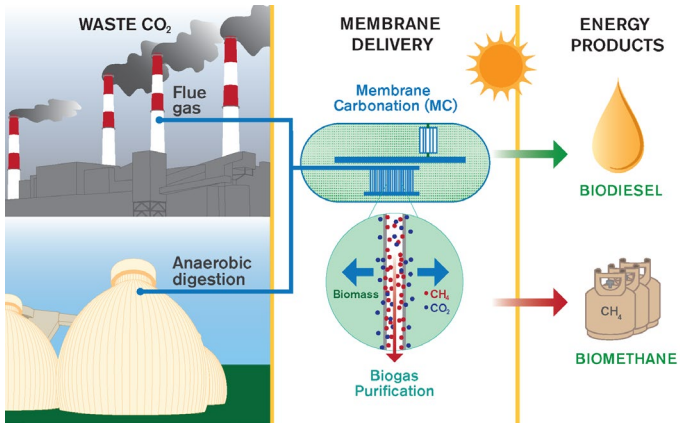

Figure 1. Schematic illustrating membrane carbonation technology for delivering CO_2 from industrial waste gases to generate microalgal biomass and renewable fuels.

The MC technology was demonstrated for cultivating microalgae in outdoor raceway ponds with 4 m^2 (43 ft^2) and 25 m^2 (270 ft^2) of aerial surface area. MC delivered the CO_2 with ~98% efficiency and with ~80% of the CO_2 utilized by the microalgae. CO_2 from biogas was delivered at high rates to cultivate the microalgae that grew at similar rates to using costly sources of 100% CO_2 and were found to provide a net savings to the microalgae farmer of 42% by significantly reducing the amount of CO_2 lost vs conventional bubbling methods. The project culminated with a final demonstration at the City of Mesa Arizona's Northwest Water Reclamation Plant (NWRP) using real biogas from the plant containing ~60% methane (CH_4), ~40% CO_2, and 250 part per million (ppm) hydrogen sulfide (H_2S) to cultivate a locally sourced microalgal species. MC and microalgae removed all odorous and corrosive H_2S from the biogas and enriched the CH_4 exiting the fibers to between 80–90% so that it can be more readily utilized as a renewable fuel or for generating electricity on demand when renewable sources are inadequate. Although some CH_4 was transferred into the microalgal reactor, a biofilm developed on the fibers that include high abundance of CH_4-oxidizing bacteria, including *Methyloversatilis*, which likely significantly reduced CH_4 that otherwise may have been released to the atmosphere. Additional research is needed to develop more selective membranes that reduce the amount of CH_4 transferred into the microalgal reactor to improve economics and reduce the net emissions.

The MC technology is poised to play a leading role in helping mitigate global CO_2 emissions. MC is particularly well suited for mitigating emission from wastewater treatment—where the microalgae capture the CO_2 emissions, grow within the wastewater itself, and utilize difficult to treat waste as a fertilizer— which will be increasingly important in areas experiencing significant drought such as the (south)western US.

Comparison of Accomplishments and Project Goals and Objectives

Project Goals

Our ultimate project goal was to demonstrate membrane carbonation (MC) outdoors using industrial CO_2 gas sources to cultivate microalgae, including synthetic and real biogas and synthetic flue gas, that achieves > 25% improvement in carbon utilization efficiency (CUE), increases microalgae growth productivity, and reduces costs. To this end, MC was demonstrated outdoors in 4-m^2 and 25-m^2 raceway ponds using synthetic flue gas and biogas as well as in 25 m^2-raceway ponds using real biogas from anaerobic digests at the City of Mesa Arizona's Northwest Water Reclamation Plant (NWRP). CUE was improved from <20% observed using conventional sparging methods to > 80% in the lab and 60% in outdoor cultivation using MC. By improving the efficiency and reducing CO_2 losses, MC further reduces cost for delivering CO_2 from $50/tonne to $9/tonne when including biomethane credits.

Project Objectives and Outcomes

The project's main objectives are described below, along with key outcomes:

1. **Solidify feasible key performance parameters** (KPP) to evaluate project success. Outcome: KPPs for each of the project tasks were identified during the initial verification meeting with Department of Energy (DOE) and National Renewable Energy laboratory (NREL) and updated during the intermediate verification.
2. **Use MC to deliver synthetic gas mixtures**, resembling multiple industrial sources, for microalgal growth. Outcome: MC was used to deliver synthetic gas mixtures with 5–80% CO_2 with a focus on flue gas (14% CO_2, 86% N_2) and biogas (35% CO_2, 65% CH_4).
3. **Achieve ≥ 50% CUE** cultivating algae with MC for ≥1 month. Outcome: Cultivation trials using synthetic biogas and flue gas showed CUE of 54–79% using flue gas and biogas.
4. **Achieve ≥ 80% CUE** cultivating algae with MC for ≥1 month. Outcome: Cultivation trials using synthetic biogas and flue gas showed CUE of 58% using flue gas and 71% using biogas. CUE can be further improved by increasing the pH setpoint and increasing the fiber surface area.
5. **Achieve ≥ 97% CH_4** product/effluent streams from synthetic biogas. Outcome: 83–95% CH_4 purity was achieved, though CH_4 losses into the liquid culture was positively correlated with purity in the effluent. CH_4 purity was highest in the morning when lower temperatures increased CO_2 solubility to be removed and O_2 levels were lowest to minimize back diffusion into the effluent gas.
6. **Deliver real biogas** using MC from an industrial source for microalgal growth. Outcome: Real biogas from City of Mesa Arizona's NWRP was used to cultivate microalgae in three 25 m^2-raceways ponds for a 9-week trial and a separate 4-week trial.
7. **10% increase in microalgal productivity** over seasonally adjusted 2016 state of technology (SOT) when grown on CO_2 delivered using MC. Outcome: Productivity increased by 21% and 35% in fall and spring using MC to deliver flue gas and 27% and 11% in fall and spring using MC to deliver biogas.

8. **Demonstrate MC reduces CO_2 delivery costs** over sparging. Outcome: MC reduces the cost for delivering CO_2 from \$50/tonne to \$9/tonne by including biomethane credits.
9. **Generate peer-reviewed reports** allowing third parties to assess the economic and technical feasibility and environmental impact of this innovative system. Outcome: Three peer-reviewed publications were published, four more manuscripts are in preparation, ten public presentations were given, and six public media reports were generated.

Key hypotheses, approaches used, and problems encountered

Key Hypotheses

Several key hypotheses for this project were:

1. Adding a bleed valve to control the rate of gas exiting the distal end of the hollow fiber will increase the rate CO_2 is delivered to the microalgae by preventing accumulation of gases not consumed by the microalgae and increase the concentration of those gases existing the fibers.
2. H_2S in biogas will be readily dissolved in the aqueous media and consumed by bacteria and thus removed from a raw biogas feedstock to increase the purity and quality of the biomethane (CH_4) exiting the fibers.
3. Increasing CO_2 transfer efficiency (CTE) along with maintaining an alkaline pH will increase the carbon utilization efficiency (CUE) of the microalgal growth system.

Approaches Used

The following approaches were used to conduct the research project for each budget period:

- Budget Period 1 [Month (M) 1–3] worked with DOE to validate and solidify feasible key performance parameters to evaluate project success.
- Budget Period 2 [M4–21] systematically performed laboratory-scale testing of MC-operating strategies with various industrial gas compositions to increase the rate of CO_2 transfer efficiency with precise pH control. Mass balances on carbon were established and quantified with mathematical modeling to help translate these methods into practice. Preliminary technoeconomic and lifecycle analyses (TEA/LCA) were performed to guide engineering design decisions.
- Budget Period 3 [M22–42] tested some of the source scenarios in small-scale (4 m^2 and 25 m^2) outdoor raceways to evaluate MC implementation in a real-world setting (e.g., with diurnal cycles, different seasons, and weather events), using actual industrial gases (e.g., real biogas from City of Mesa Arizona anaerobic digesters) and gain experience that will lead to effective scale up in the future. TEA and LCA models were revised to account for data collected during outdoor testing and will inform decision-making for how best to move MC beyond Technology Readiness Level (TRL) 4 toward commercialization.

Problems Encountered

Several challenges were encountered throughout the project as noted below:

- Outdoor trial #1 was cancelled due to COVID-19 mitigation policies at ASU & AzCATI.
- Microbial contamination and culture crashes were pervasive with *Scenedesmus obliquus* UTEX 393 during the hot summer months for Outdoor trial #2. Hence, the team switched to using *Picochlorum celery* (Pico), a very fast-growing saltwater strain, which grew very well. Pico grew so well the MC modules were not able to deliver sufficient CO_2 since they were sized for the slower growing *Scenedesmus* strain; thus, the cultures grew slightly slower than cultures growing with sparged pure CO_2.
- CO_2 transfer was inadequate with flue gas (14% CO_2), leading to carbon-limited growth.
- Leaks in the membranes were observed when cultivating during the hot summer months. We hypothesize that the leaks were due to differences in temperature when the epoxy used to bind the fiber modules were assembled (room temperature) and the hot outdoor temperatures (~40°C) during cultivation.
- Because of delays during outdoor trial #2, outdoor trial #3, planned for fall 2020, would not have started until December. Hence, it was cancelled, since it would have been similar to the scheduled winter trial in February.
- The 25-m^2 pond vendor failed to deliver the ponds that were ordered. The team was able to build three 25-m^2 ponds that worked very well, but the delivery failure delay led to the decision to cancel of the final 25-m^2 trial at AzCATI and instead increase the scale of the trial at the City of Mesa using real biogas from 4-m^2 to 25-m^2 ponds, which worked very well.
- Mitsubishi Rayon fibers were not able to achieve CH_4 effluent purity of ≥ 97% required for pipeline natural gas and the target CO_2 flux of 400 g m^{-2} d^{-1}, while also keeping the levels of CH_4 transferred through the membrane into the cultivation medium low enough to meet the renewable fuel standard (RFS). Methane release to the atmosphere was at least partially mitigated because it was consumed by methanotrophic bacteria, including *Methyloversatilis*, in the medium before the CH_4 was released to the atmosphere.
- Some O_2 generated during microalgal photosynthesis back diffused into the hollow-fiber lumen, which limited the purity of the CH_4 in the biogas product stream to 85–90%.
- COMSOL multi-physics simulation software was not able to represent the chemical speciation of CO_2 to HCO_3^- or CO_3^{2-} in the bulk liquid, which provides additional driving force for CO_2 diffusion, and thus underestimated the CO_2 flux by 4-fold compared to experiment. The team increased the CO_2 mass transfer coefficients to get around this limitation and able to closely approximate experimental values.
- Some biofouling was observed on the MC modules during cultivation trials at the City of Mesa. Biofouling reduced CO_2 flux, but it also helped reduce O_2 back diffusion to maintain higher effluent CH_4 purity (~85%) during the day when O_2 production was highest.

Summary of activities and key outcomes

A summary of each research activity and key outcomes is now presented in the order of the defined tasks. This is not an exhaustive compilation of all work performed, and more details can be found within the team's quarterly reports.

Task 1 - Process and Data Validation. [Go/No Go]

The ASU and Sustainability Science LLC team worked with advisors from DOE and NREL advisors who visited ASU to assess the technology readiness level (TRL) of the key technologies and key project metrics.

Key Outcomes: Feedback from DOE and NREL was used to update the budget, statement of project objectives, and technical datasheet accordingly and leading to a Go approval to advance to budget period 2.

Task 2 – Abiotic evaluation of MC delivery rates using CO_2 and other gases

We evaluated MC performance using the mixed gas streams representative of different industrial CO_2 streams, as summarized in **Table 2.1**. To obtain > 95% carbon transfer efficiency ($CTE_{abiotic}$), we added and adjusted a flow restrictor at the distal end of the fibers to understand the relationship between CO_2 flux and $CTE_{abiotic}$. We present the results for two scenarios: (1) $CTE_{abiotic}$ for CO_2 streams without CH_4 and (2) CH_4 upgraded and $CTE_{abiotic}$ for biogas.

Table 2.1. The compositions of gas streams in the range of 5 to 80% CO_2 in the study

Gas Mixture	CO_2%	N_2%	O_2%	CH_4%
80/20	80	20	-	-
50/50	50	50	-	-
Biogas	35	-	-	65
Combust Bio	25	65	10	-
Flue gas 14%	14	81	5	-
10%	10	71	19	-
Flue gas 5%	5	85	10	-

Flux and CTE in abiotic tests (exclusive of biogas)

Figure 2.1 (a) summarizes abiotic CO_2 fluxes with 0 (closed end), 0.2, or 2 cm^3/min (restricted flow) from the membranes' distal end effluent when the CO_2 concentration in the input gas was from 5% to 80% and delivered at 10 psig total gas pressure. A lower concentration of CO_2 in the input stream always led to a lower CO_2 flux: e.g., 10% CO_2 had a flux roughly 20-fold lower than for 80% CO_2 when operated with the restricted flow rate of 2 cm^3/min. Further restricting the exit flow rate from 2 to 0.2 cm^3/min showed a larger flux decline than going from 0.2 to 0 cm^3/min, which shows that further research needs to evaluate the required flow to sufficiently flush inert gases from the distal end.

Figure 2.1 (b) shows that all tests with 0.2 cm^3/min restricted-flow and closed-end operations had $CTE_{abiotic} \geq 99\%$. Tests with 2 cm^3/min restricted flow gave > 95% of $CTE_{abiotic}$ for 5 to 50% CO_2 streams, but the 80% CO_2 stream achieved only 85% $CTE_{abiotic}$. Higher CO_2 streams may require more severely restricted flow to achieve >95% of $CTE_{abiotic}$, although increasing driving force (i.e., total gas pressure) also increased the flux of CO_2 into the media (data not shown). Results from completely open-end studies (Shesh et al.,2019; Lai et al., 2020)[1,2] showed that the CO_2 flux was approximately linear with $\%CO_2$ content, but $CTE_{abiotic}$ was < 1 % due to the very high exit flow rate (> 1400 cm^3/min). Thus, restricted flow created a trade-off between CO_2 flux and $CTE_{abiotic}$, which also was noted by Lai et al. (2020) for 10% CO_2.

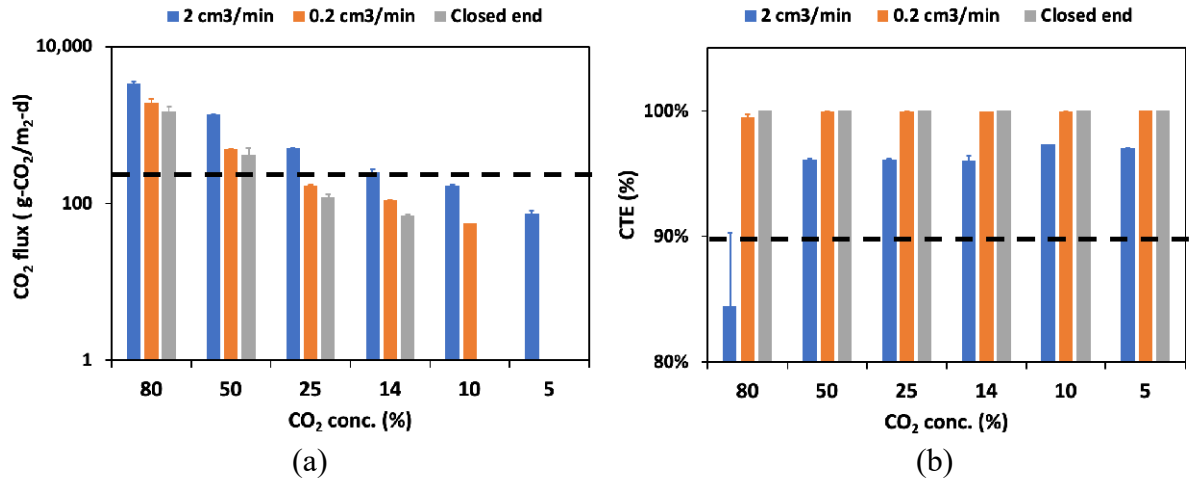

Figure 2.1. (a) CO_2 flux obtained from 5 to 80% CO_2 gas streams. (b) Carbon transfer efficiency (CTE) obtained from 2 or 0.2 cm^3/min (sccm) restricted flow, as well as from complete closed end using 5%- to 80%-CO_2 gas streams. Dashed line represented the target flux at 250 g/m2/d and 90% CTE, respectively. Data for the 10%-CO_2 gas stream were adapted from Lai et al. (2020) for comparison.

CH_4 upgrade and loss across the membrane wall for biogas

We investigated the tradeoff between CH_4 purity of residual biogas exiting the distal end of the hollow fibers vs CH_4 loss across the fiber walls into the liquid medium. Our goal was to achieve $\geq$ 97% CH_4 in the effluent while keeping CH_4 transfer to the medium to $\leq$ 1 % of the total CH_4 in the biogas. The main variables evaluated were the length of the fibers by comparing 15 cm and 30 cm bundles; the total surface area of the fibers including bundles of 4 fibers and bundles of 32 fibers of a fixed 15 cm length; and varying the delivery from 2.5 to 25 psig while holding the effluent flow to a constant 5 cm^3/min and varying the effluent flow from 2.5 to 20 cm^3/min while holding the delivery pressure constant at 10 psig. The results, in **Figure 2.2(a)**, show that $\geq$ 97% CH_4 effluent could be obtained with at least 20 psig pressure, but this resulted in $\geq$ 11 % of the CH_4 transferred and lost across the membrane wall. At the lowest pressure tested, 2.5 psig, only 3% of the input CH_4 was transferred, suggesting even lower pressures may be needed to reduce CH_4 transfer through the fibers to meet the target of $\leq$ 1%. With the lower surface area bundle (4 fibers), CH_4 transfer below $\leq$ 1% could be achieved; however, CH_4 effluent purity was only increased up to 75% at 25 psig.

Figure 2.2 (b) shows results from varying the effluent flow from 2.5 to 20 cm^3/min with the constant pressure supply at 10 psig to evaluate CH_4 transfer and loss across the wall. The results suggest that the lower effluent flow of 2.5 cm^3/min was needed to achieve an effluent CH_4 purity ≥ 95%, but it led to higher CH_4 transfer across the membrane wall. In contrast, higher effluent flow of 20 cm^3/min reduced CH_4 transfer across the membrane to ≤ 1%, but CH_4 effluent purity was only just above 70%.

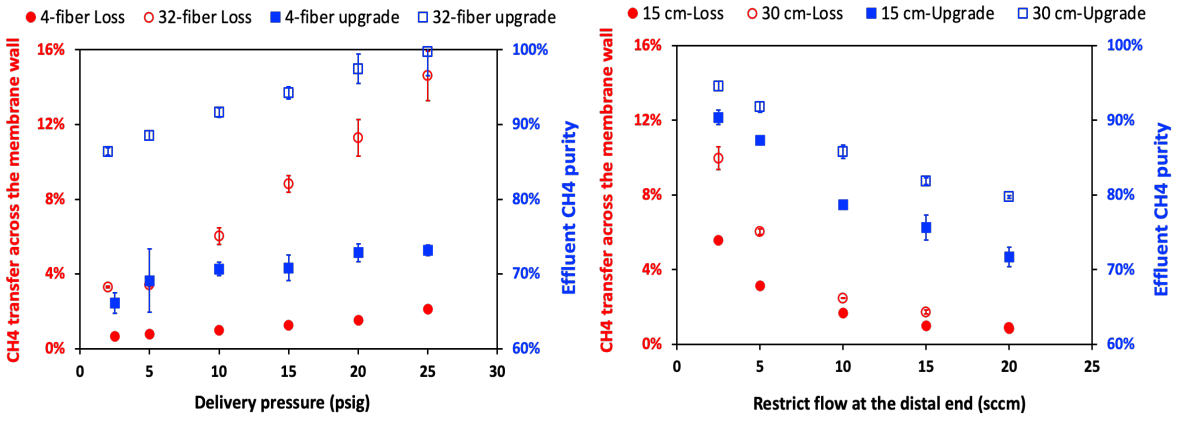

(a) (b)

Figure 2.2. Optimizing bleed-valve operation for CH_4 purification for biogas. The scenarios evaluated included (A) flow restricted to a constant 5 cm^3/min and varying the delivery pressures from 2.5 to 25 psig; and (B) holding a constant 10 psig pressure while varying the effluent flow from 2.5 to 20 cm^3/min.

Flux and $CTE_{abiotic}$ for biogas

Using the same experimental setups, we report how delivery pressure and restricted flow affected CO_2 flux and carbon transfer efficiency ($CTE_{abiotic}$). The two sets of variables were evaluated including (a) fiber surface areas between 4-fiber bundle and 32-fiber bundle with a fixed 30-cm fiber length and (b) length of fibers between 15 and 30 cm with 32 fibers per bundle. We evaluated the case (a) with a constant restricted flow of 5 cm^3/min, while varying the pressure from 2.5 to 25 psig; and (b) with a constant pressure of 10 psig but varying the effluent flow from 2.5 to 20 cm^3/min.

Figure 2.3(a) shows that CO_2 flux and CTE were positively correlated with delivery pressure, i.e., higher pressure led to higher CO_2 flux and CTE. However, fiber bundles with more surface area were far superior for achieving high CO_2 transfer efficiency, with 85−100% CTE observed at 2.5 psig, which was much better than bundles with lower surface area (4 fibers) that only got up to ~72% CTE at 25 psig. **Figure 2.3 (b)** shows CO_2 flux and CTE from varying the effluent flow in the bleed valve from 2.5 to 20 cm^3/min with the constant pressure supply at 10 psig. CTE was negatively correlated with the effluent flow, i.e., lower effluent flow led to higher CTE for two fiber lengths, but longer length consistently showed higher CTE compared with short fibers. With effluent flows up to 5 cm^3/min, CO_2 flux increased with the effluent flow. The CO_2 flux started to plateau or even declined when effluent flow was greater than 10 cm^3/min, suggesting more CO_2 was lost through the effluent instead of going into the media. A poor flux

reflected a poor CTE. It is worth noting that the CO_2 flux for biogas was above our project target of 400 g/m^2/day in all cases.

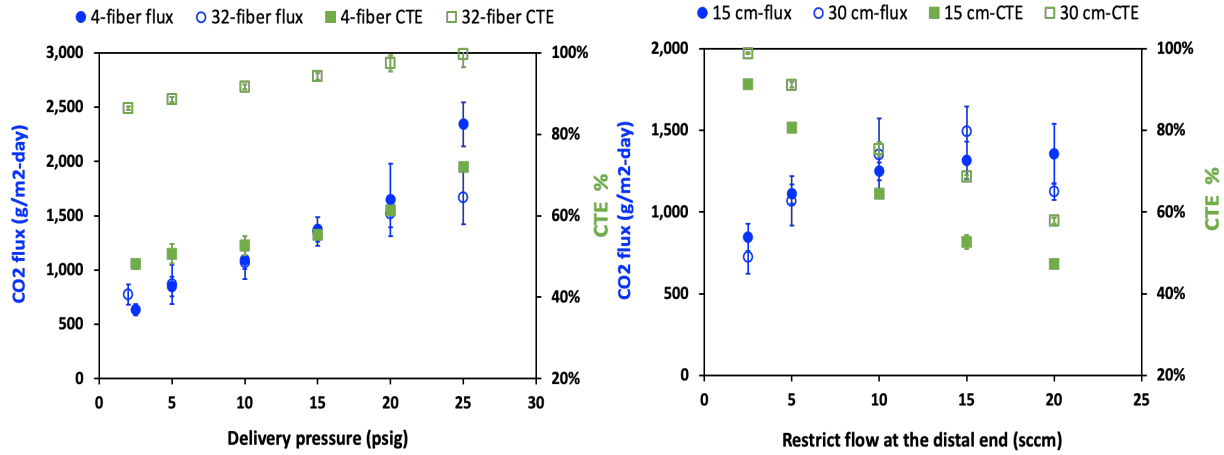

(a) (b)

Figure 2.3. Optimizing bleed-valve operation for CO_2 flux and carbon transfer efficiency for biogas. The scenarios evaluated included (A) flow restricted to a constant 5 cm^3/min and varying the delivery pressures from 2.5 to 25 psig; and (B) holding a constant 10 psig pressure while varying the effluent flow from 2.5 to 20 cm^3/min.

CH_4 loss validation

We investigated CH_4 lost across the membrane wall by manually measuring the CH_4 within the headspace of the closed bioreactor and effluent of the fiber lumen. A gas flow meter is a convenient tool for estimating mass balance, but its measurement accuracy is not sufficient at the small flow rates required during indoor cultivation trials (i.e., < 2.5−20 cm^3/min). Therefore, we developed a more robust method to calibrate the gas flow meter readings using a Total Organic Carbon (TOC) analyzer (Tekmar Lotix, USA) to measure CO_2 flux. Given the known gas composition of the inlet gas we can then determine the inlet flow of CH_4 into the fibers and obtain a CH_4 mass balance and validate against the CH_4 loss obtained by manually collecting gases in a bag and measuring its composition using gas chromatography (GC). Our approach is summarized in **Figure 2.4**. The results, summarized in **Table 2.2**, indicate that CH_4 loss obtained using the measured gas flow revised by TOC readings was very close to our more comprehensive manual measurement using GC of the CH_4 partition in the gas and liquid phase of the reactor as well as the effluent CH_4 coming out the fiber lumen. The errors in the raw gas flow meter readings were likely due to the small flow, digital meter drift, and no option to compensate the gas readings for a customized gas mixture. Therefore, any small variations could amplify errors. The developed method for calibrating the gas flow meter readings using TOC also enabled is to correct data collected previously.

Table 2.2. Comparison of CH_4 loss values obtained from three different approaches

CH4 loss estimation	Flow meter method	TOC revised flow method	Manual method
Test#1	30.8%	5.7%	6.5%
Test#2	33.9%	4.8%	5.5%

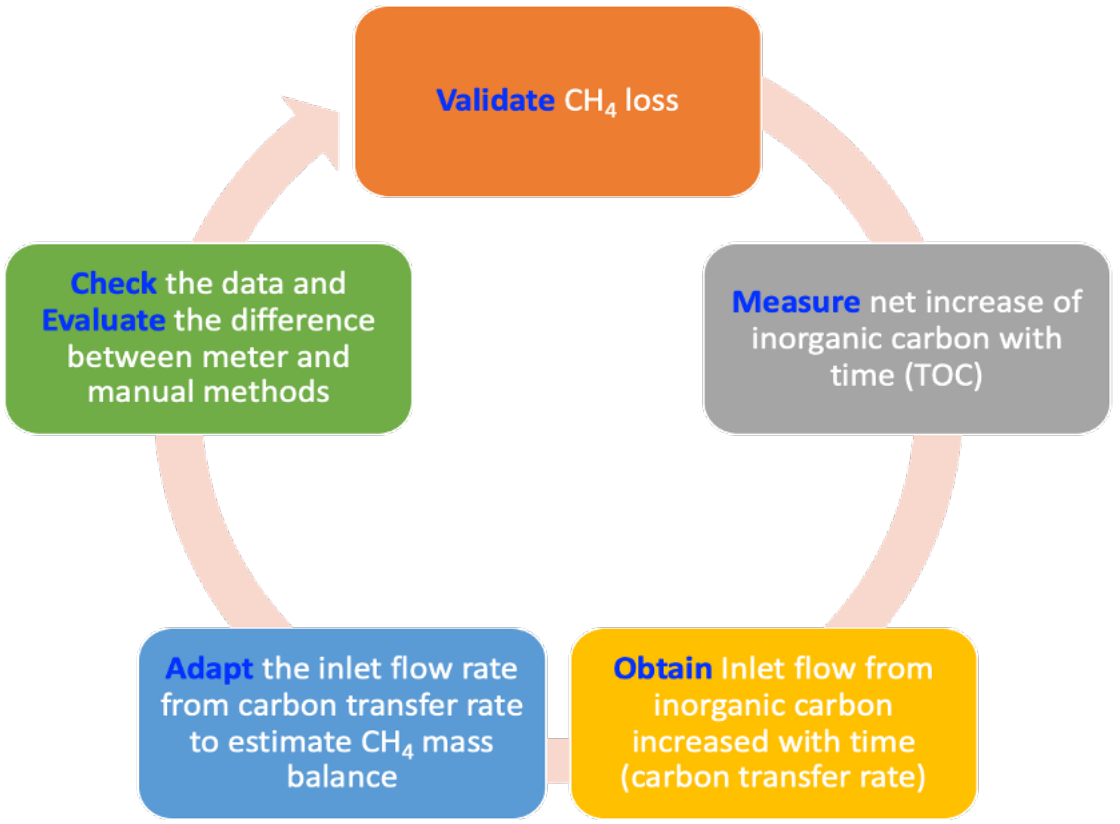

Figure 2.4. CH_4 loss validation method: (1) measure CO_2 flux using the Total Organic Carbon (TOC) Analyzer; (2) obtain the inlet gas flow rate using the measured CO_2 flux; (3) adapt the inlet gas flow rate to estimate the CH_4 balance, (4) compare the two methods and (5) validate CH_4 loss across the wall using gas chromatography.

Removing corrosive H_2S removal using MC

In addition to CO_2 and CH_4 transfer across the membrane, H_2S present in the biogas is also a key compound to be captured during biomass cultivation. Biogas was synthesized with 200 and 400 ppm of H_2S blended with N_2 gas and evaluated to see whether H_2S could be delivered across the fiber membrane into the media and removed from the effluent as an indication of what could be expected during subsequent biological testing. Gases containing 200 and 400 ppm H_2S (Matheson, USA) were set to 10 psig (69 kPa-gauge supplied pressure) for the tests, and polyurethane tubing (Surethane NSF-51, ATP, USA) was used to connect the gas line. The outlet (bleed) valve flow restriction was set as 5 cm^3/min by a flow controller (MC Series, ALICAT Scientific, USA). The flow meter (MC Series, ALICAT Scientific, USA) was installed before the fiber bundle and a flow controller was sequentially connected to the fiber bundle. The fiber bundle contained 32 fibers with ~27-cm fiber length, corresponding to 0.016 m^2 surface area. The test was conducted in 1-L bottle with the closed system (without headspace) filled with 1.125 L of 5 mM $NaHCO_3$ in distilled water (**Figure 2.5**). Periodically,

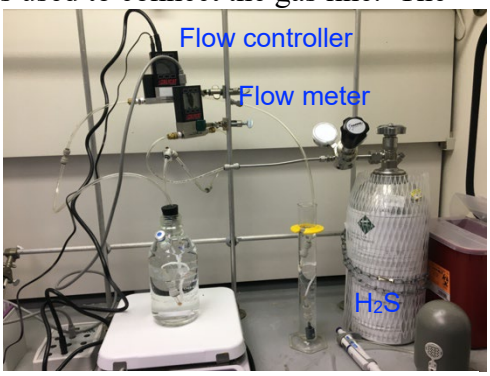

Figure 2.5 H_2S-capture setup

duplicate 4-mL aliquots were withdrawn for the H_2S measurement after 1, 2, 4 and 6 hours, and replaced with 8 mL of fresh 5 mM $NaHCO_3$. The gas outlet was connected to the one fiber bundle (32 fibers, 13 cm length) and one small sparger that was placed in the 250 mL graduated cylinder filled with 250 mL of 5 mM $NaHCO_3$. A 4 mL-aliquot was taken at the same period above. The H_2S delivery rate across the membrane was computed and summarized in **Table 2.3**. Based up the gas flow rate (5 cm^3/min), the estimated delivery rate matched well with the measured delivered rate, indicating nearly 100% of H_2S was captured by the medium, as H_2S was not present above the detection limit in the exiting gas.

Table 2.3 H_2S delivery rate via hollow-fiber membrane

H_2S concentration (ppm)	Computed delivery rate (mg/hr)	Measured delivery rate (into the media, mg/hr)	Captured ratio (%)
200	0.084	0.084 ± 0.005	~100%
400	0.168	0.160 ± 0.011	~95%

Key Outcomes:

Two key findings were learned in Task 2: (1) More surface areas and/or lower effluent flow enhanced the CTE and CH_4 transfer across the wall. (2) Lower delivery pressure (at 2.5 psig) could lower CH_4 (< 4%) transfer across the fiber wall. These two trends can help us optimize CTE with the least amount of CH_4 transferred across the membrane wall. (3) 100% of H_2S was removed from a gas comprising input 200 ppm H_2S (a realistic level in digester biogas).

Task 3 – Evaluate indoor biological cultivation with MC using synthetic gases

Flue gas and biogas were evaluated as a CO_2 source for cultivating microalgae at the bench scale. We varied the gas supplied pressure from 10 psig up to 15 psig for flue gas and biogas in order to improve the CO_2 flux. Also, a key factor for efficiently removing CO_2 from the inlet gas stream is a significant uptake from the microalgae. The existing indoor cultivation setup had a rather low light intensity that limited algal growth. CO_2 in the fiber lumen needs to be depleted to achieve higher CTE and CUE. Thus, we increased light intensity up to 112 and 208 µmol photons m^{-2} s^{-1} fluorescent illumination for the flue gas and biogas setup, respectively, in order to raise up the biomass productivity to more effectively capture CO_2 and deplete CO_2 in the fiber lumen. For the flue-gas study, we kept the same numbers of fibers (32 fibers), but extended the fiber length up to 28 cm from 15 cm in order to deplete CO_2 further in the fiber lumen. For the biogas study, we also used 28-cm fibers, but increased the outlet flow a bit more, from 0.75 to 1.6 cm^3/min, in order to reduce CH_4 transfer into the culture media.

Cultivation using flue gas

Indoor cultivation trials were conducted using diurnal conditions integrated with a pH-stat system mixing at 450 rpm, and with the temperature held at 25–26°C. *Scenedesmus obliquus* UTEX 393 was used as an inoculum. The BG-11 medium was delivered at 300 mL/d with a 6-d solid retention time (SRT) for biomass growth. **Figure 3.1** shows biomass productivity with flue gas was almost identical to cultivation with 100% CO_2, indicating that using flue gas CO_2 streams did not affect biomass growth. The carbon transfer efficiency (CTE) and carbon utilization efficiency (CUE) can be achieved as 97 ± 2 and 81 ± 4, respectively (**Table 3.1**) by measuring 1) the total carbon in the biomass dry weight, 2) the net total carbon in the liquid media using a Lotix combustion TOC analyzer (Teledyne Tekmar, OH, USA) whenever new growth medium was added, and 3**)** the effluent CO_2 concentration along with flow rate. It is

worth noting that the low CTE and CUE value for 100% CO_2 occurred because the fibers optimized for delivering dilute CO_2 streams was used for 100% CO_2, leading to a drop in pH that

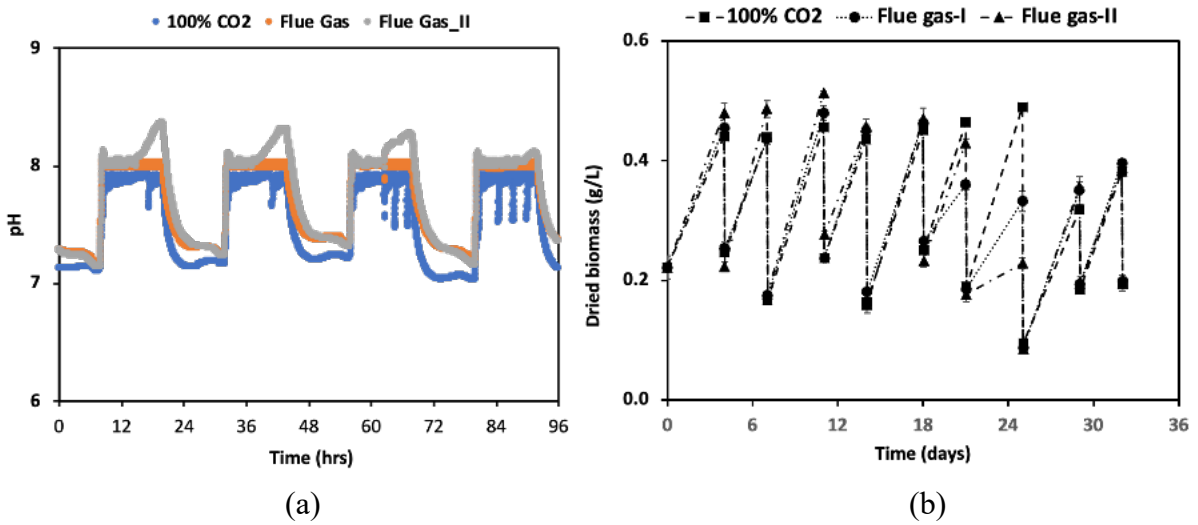

(a) (b)

Figure 3.1 The semi-continuous cultivation was maintained for over 4 weeks. 100% CO_2 was tested as the baseline comparison.

reduces biomass growth; we have previously established methods to deliver 100% CO_2 with near 100% efficiency using MC technology.[3]

Table 3.1 Parameter and performance set for flue gas evaluation

	100% CO_2	Flue Gas
Light intensity	112	112
Biomass productivity (mg/L-d)	70 ± 10	70 ± 10
Pressure (psig)	5	15
32 Fibers (14 cm length)	1 bundle	2 seq. bundle
Fiber surface area (cm^2)	39	79
Flow at the distal end (sccm)	920	2
Effluent CO_2 (%)	100 %	< 1% *
Duration of venting (min/d)	1.2 ± 0.6	668 ± 35
Carbon transfer efficiency (%)	15 ± 8	97 ± 2
Carbon utilization efficiency (%)	12 ± 5	81 ±4

* Most of time during cultivation conditions, except for some occasional spikes between 1–5% CO_2 during the first few hours after the light was turned on. See **Figure 3.2**.

Figure 3.2 shows the effluent CO_2 concentration for flue gas supplied at 15 psig with 28-cm fiber length. Effluent CO_2 was maintained below 1% during most of cultivation period, except for a few hours after the light was switched on. We hypothesize this is because the concentration of CO_2 in the effluent depended on the rate of CO_2 removal by the microalgae, which increased as the biomass grew after the light was turned on each morning.

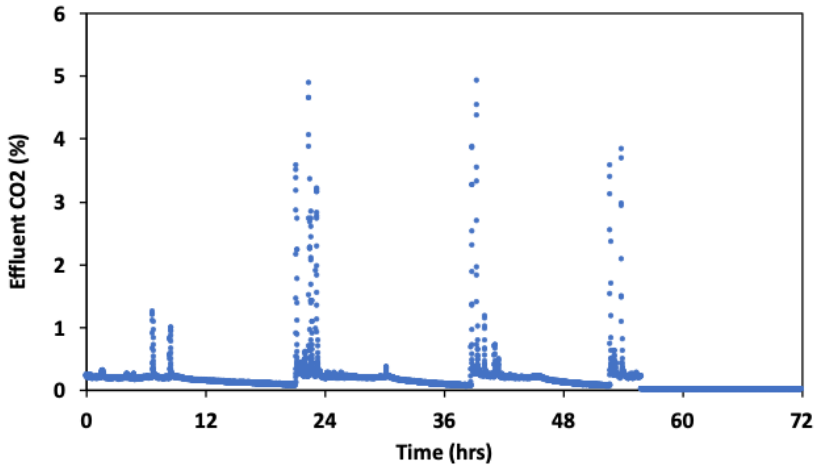

Figure 3.2 Effluent CO_2 concentration for flue gas supplied at 15 psig with 28 cm fiber length.

Indoor cultivation using biogas

Figure 3.3 shows biomass productivity with synthetic biogas had almost identical growth rates as with 100% CO_2, indicating that biogas streams did not affect biomass growth. The carbon transfer efficiency (CTE) and carbon utilization efficiency (CUE) were as high as 99 ± 0.1 and 82 ± 1, respectively (**Table 3. 2**). Since the cultivation was in an open system, it was difficult to determine exactly how much CH_4 was transferred into the medium. **Figure 3.4** shows the effluent compositions during biogas cultivation. Nearly all CO_2 delivered to the fibers was removed by the microalgae, leaving mostly CH_4; however, a significant amount (up to ~15%) of O_2 back diffused into the lumen as a byproduct of photosynthesis. Thus the ~98% CH_4 achieved in the fiber effluent during abiotic testing with identical parameters could not be reproduced during cultivation. Actively removing O_2 from culture media during cultivation (i.e., outdoor cultivation) might reduce the amount of O_2 transferred and improve the quality of the CH_4 in the effluent

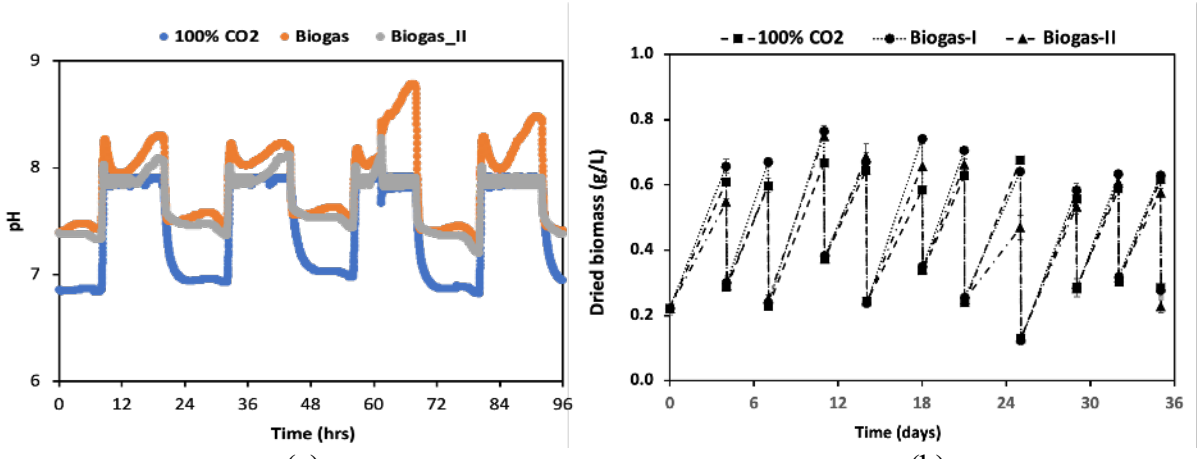

(a) (b)

Figure 3.3. The semi-continuous cultivation was maintained for over 4 weeks showing the pH (a) and dry biomass (b). 100% CO_2 was tested as the baseline comparison.

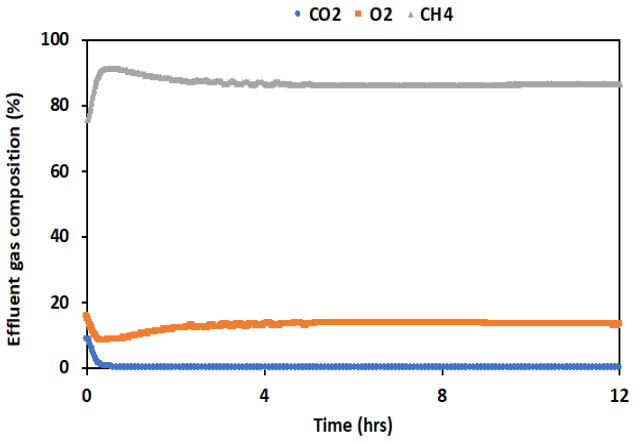

Figure 3.4. Compositions of effluent gas was obtained according to a K33 BLG 30% CO_2 sensor (CO2Meter.com, FL, USA) and a UV Flux 25% oxygen sensor (CO2Meter.com, FL, USA). The CH_4 concentration was obtained from the computed values and compatible to the range obtained from GC-TCD assay as summarized in Table 3.2. N_2 gas was not detectable above the detection limit of GC-TCD.

Table 3.2. Parameter and performance set for biogas evaluation

Open to atmosphere condition	100% CO_2	Biogas
Light intensity	208	208
Biomass productivity (g/L-d)	100 ± 10	110 ± 10
Pressure (psig)	10	15
16 Fibers (~14 cm)	1 bundle	1 bundle + 1 bundle with 4 fibers
Fiber surface area (cm^2)	20	25
Flow at the distal end (sccm)	937.5	0.75
Effluent CO_2 (%)	100%	<1 %
Duration of venting or bleed (min/d)	17.5 ± 16.7	< 12 hrs
Carbon transfer efficiency (%)	9 ± 13	98 ± 0.1
Carbon utilization efficiency (%)	7 ± 11	82.0 ± 0.8
CH_4 (%)	N.A.	84.5 ± 4.7
O_2 (%)	N.A.	14.7 ± 2.2
N_2 (%)	N.A.	<1 %

We also evaluated the ability of the existing microbial community to consume H_2S and CH_4 that was transferred across the membrane wall. The operation parameters are summarized in **Table 3.3**. Each parameter was evaluated for at least two weeks, and the data were averaged from at least triplicate results. We cultivated the biomass with biogas blended with 200 ppm H_2S and along with 100% CO_2 a control for comparing the productivity. The control biomass was sustained for two months with consistent biomass productivity.

Table 3.3 Parameters for indoor biological cultivation using MC (Closed system)

Biogas blended with 200 ppm H_2S	Test#1	Test#2	Test#3	Test#4
Light intensity ($\mu E/m^2.s$)	208	208	208	208
Inlet Pressure (psig)	15	~4.75	~4.25	~4.15
Fibers	16 plus 4	16 plus 4	16 plus 4	16 plus 4
Fiber surface area (cm^2)	25	25	25	25
Distal end with restricted flow (sccm)	1	1.2	1.4	1.6

The results of these experiments are summarized in **Figure 3.5.** They show (1) ~10% lower biomass productivity (vs control (open cultivation), ~0.12 g/l-d); when lower pressure (4−5 psig) was supplied due to carbon limitation; (2) nearly 100% of the H_2S was removed in all scenarios and H_2S was not detected in the headspace (<< 1 ppm detection limit using a dragger tube); (3) CH_4 could be enriched in the fiber effluent up to 87% with 15 psig and 1 cm^3/min, but CH_4 in the effluent could still be enriched up to 80% at lower pressure (i.e., 4−5 psig) with 1.2 to 1.6 cm^3/min; (4) when the pressure was reduced and effluent flow was increased, CTE and CH_4 across the membrane wall started to decline from 95% to 65% and from 22% to 13%, respectively; (5) Based on the CH_4 mass balance, 13−26% of the CH_4 input to the fibers was transferred into the medium and 5−10% may have been consumed by microbes within the culture.

According to the DNA-sequencing outcomes obtained from open cultivation (**Figure 3.6**), the CH_4 consumption might not fully depend on bacteria but perhaps also by fungi. H_2S-oxidizing bacteria were not present in the sequencing outcomes, and the observed complete H_2S removal may be ascribed to the direct oxidation by O_2 generated from photosynthetic process.

Microbiome

The microbial community within the medium after cultivation with flue gas and biogas (without H_2S) was analyzed, and the results are shown in **Figure 3.6**. The microbial communities did not shift significantly with gas composition, but the communities clearly shifted from day zero of the cultivation. We hypothesized that the presence of CH_4 in the medium would select for microorganisms that consume CH_4. However, methanotrophic bacteria were not prominent. The relevant methanotroph was *Methylophilu*s, which was present when delivering the biogas stream and pure CO_2, implying that its presence may not be directly associated with CH_4. Among the aerobic bacteria, phylotypes most closely related to *Shinella* sp. DD12, a bacterium that enables phosphite assimilation was observed, and it likely was competing with the algae for phosphorus within the BG-11 media.[4] Phylotypes most closely related to *Pseudomonas* and other

heterotrophic aerobic bacteria (i.e., *Hyphomonas, Hydrogenophaga, Brevundimonas*) were present, which is commonly observed with algal biomass, since the algae release organic compounds. Species of fungi, *Mitosporidium daphnia* (up to 78% abundance of fungi), fungal sp. Mo6-1 (up to 24% abundance of fungi), and *Polychytrium aggregatum* (up to 5% abundance of fungi) were identified in all the samples, and the presence of fungi suggests that they played a role in metabolizing organic compounds generated from algal biomass or CH_4 provided from biogas.

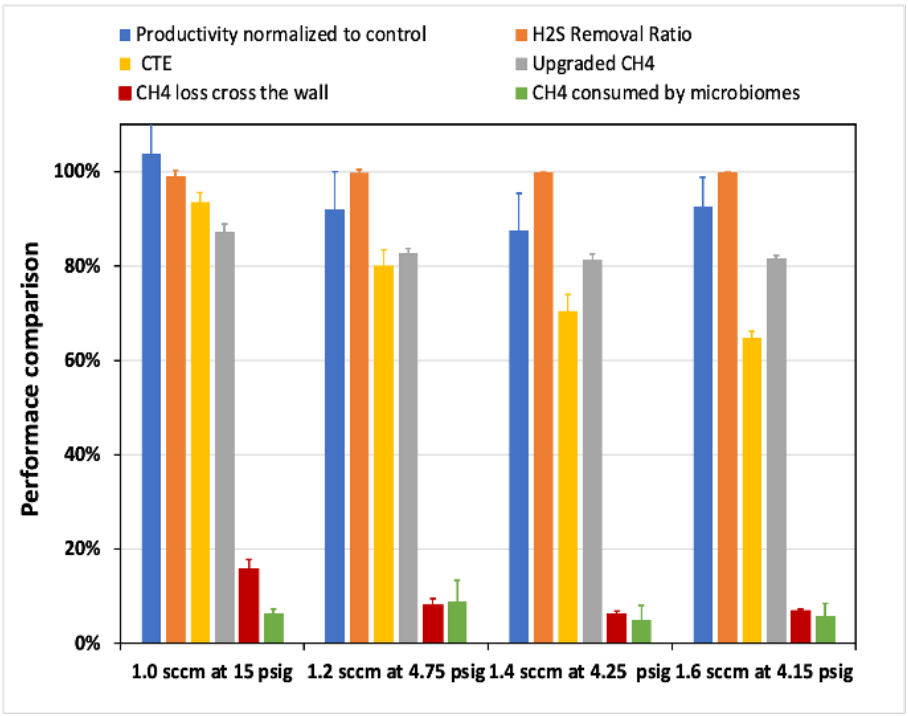

Figure 3.5 Performance of indoor biological evaluation at different operating scenarios (closed system).

Key Outcomes: (1) Given our approach using a bleed valve and pH-actuated venting at fiber's distal end, continuous cultivation with *Scenedesmus* using flue gas (14% CO_2) could achieve 97 ± 2% CTE_{biotic} and 81 ± 4 % CUE during a cultivation trial that lasted over 4-weeks. (2) With a continuous bleed approach with the flow restricted to 0.75 cm^3/min, *Scenedesmus* using biogas

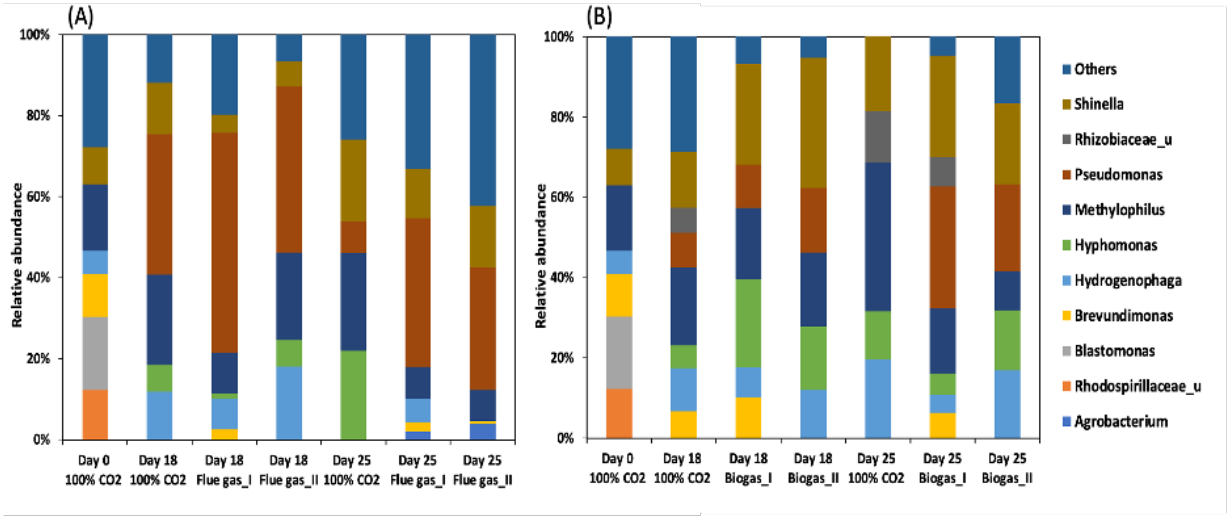

Figure 3.6. 16S rDNA gene amplicon sequencing. Analysis presented at the genus level obtained from indoor cultivation using (A) flue gas and (B) biogas streams.

(35%/65% CO_2/CH_4) could achieve 98 ± 0.1 % CTE_{biotic} and 82 ± 0.8 % CUE during a cultivation trial that lasted over 4-weeks; lower gas pressure (4.15–4.75 psig) and higher restricted flow (1.2–1.6 cm^3/min) could reduce CH_4 loss across the membrane wall to ≤ 6 %, although the CTE also was reduced; (3) O_2 intrusion into the membrane lumen was identified and associated with a high CTE (higher CTE led to higher O_2 intrusion); (4) nearly 100% of the H_2S was removed during cultivation; and (5) microbes in the culture consumed some of the CH_4 transferred across the membrane to at least partially mitigate its escape to the atmosphere.

Task 4 – Mathematical modeling of MC gas transfer

We developed a 2-D model in COMSOL, including adding the basic MC-membrane design into the program and identifying the required modeling modules for the system. The COMSOL model was developed to simulate CO_2 delivery from biogas fed into the membrane lumen, with the goal of achieving ≥ 97% effluent CH_4 concentration exiting the lumen at the terminal fiber end. The model configuration is shown in **Figure 4.1**, and baseline modeling parameters are summarized in **Table 4.1**. The COMSOL model includes steady and non-steady-state gas and liquid transport and diffusion based on Fick's law, allowing it to describe diffusion across the multiple boundary layers between the gas in the lumen and the bulk liquid outside the membrane.

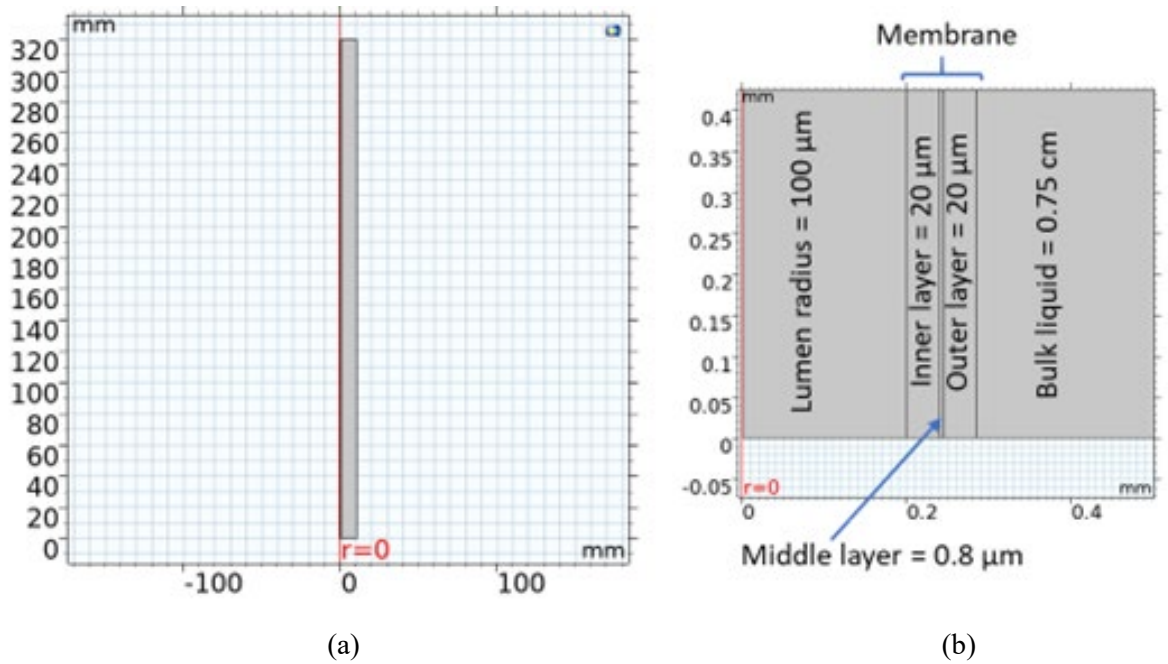

(a) (b)

Figure 4.1. Diagrams of system modeled in COMSOL: (a) high-level view of the fiber immersed in bulk liquid and (b) detailed view of the different layers within the fiber as seen at the biogas influent end.

The COMSOL model consisted of 5 different sections as summarized in Table 4.1: (1) the membrane lumen; the membrane wall' (2) inner macroporous layer, (3) middle nonporous layer, and (4) outer macroporous layer; and (5) the bulk liquid outside the membrane. Membrane dimensions were based on the Mitsubishi-Rayon membrane data sheet. The COMSOL model consisted of two modules to describe the different physical, transport, and chemical phenomena: Laminar Flow (LF) and Transport of a Diluted Species (TDS). The LF module described

fluid/gas flow and, therefore, produced a velocity gradient profile through the bulk liquid and lumen. For this module, the flow rate at the influent and the pressure at the effluent were specified with an additional pressure boundary constraint implemented at the influent to maintain a constant pressure across the system, as observed during the experiments. Second, TDS used the velocity profiles obtained in the LF module to describe the combined effects of diffusion and convection in all sections of the system. TDS also requires specification of the initial concentrations, operating concentrations, membrane porosity (where appropriate), and all diffusion coefficients to develop a complete model of the system.

Table 4.1. Baseline model-simulation parameters

Parameter	Dimensions	Value	Source
Number of membrane fibers	--	32	Experimental data
Membrane length	mm	305	Experimental data
Lumen radius	μm	100	Mitsubishi
Membrane thickness			
Inner layer	μm	20	Mitsubishi
Middle layer	μm	0.8	Mitsubishi
Outer layer	μm	20	Mitsubishi
Membrane porosity	--	0.43	Ahmed et al. (2004)
Bulk liquid thickness	cm	0.75	--
Biogas influent composition			
CH_4	% (mg/L)	65 (711)	Experimental data
CO_2	% (mg/L)	35 (1053)	Experimental data
O_2	mg/L	0	Experimental data
Biogas influent flow rate	sccm	9.5	Experimental data
Biogas effluent flow rate	sccm	9.5	Experimental data
Biogas pressure in lumen	psia	24.4	Experimental data
Bulk liquid flow rate	L/min	100	Experimental data
Bulk-liquid initial concentrations			
CO_2	mg/L	0	Experimental data
CH_4	mg/L	0	Experimental data
O_2	mg/L	0	Experimental data

The first set of simulations was based on indoor biogas experiments. These experiments focused primarily on CH_4 and CO_2 diffusion into the bulk liquid. For the data presented here, biogas consisted of 65% CH_4 and 35% CO_2. The lumen's biogas flow rate was restricted to 5.5 sccm at the outlet and had a constant pressure of 24.4 psia at all locations across the membrane. The membrane bundle consisted of 32 membranes. To simulate constant CO_2 depletion in the bulk

liquid (from the microalgae), the bulk liquid was assumed to flow concurrently with the lumen flow at a rate of 100 L/min parallel to the outer surface of the membrane wall. The model did not reflect the liquid volume of an actual reactor or a mass balance in the bulk liquid. The model was run for non-steady state conditions for 100 hours of simulated operation from start up.

For these initial modeling runs, experimental diffusion coefficients were not available. Diffusion constants for the biogas and bulk liquid were based on literature values for mixed biogas and gases in liquids and are summarized in **Table 4.2**. Since the membrane has a moderately high porosity (43%) in the inner and outer layers, the diffusion constants in the inner membrane layer were assumed to be the same as the gas diffusion constants. The macropores of the outer membrane layer were assumed to be saturated with the bulk liquid; therefore, the diffusion constants in the outer layer are the same as the diffusion constants in the bulk liquid. Diffusion constants through the nonporous middle layer were assumed limiting the system and, as a baseline, were assigned values based on preliminary modeling and initial experimental data.

COMSOL provided a consistent and reliable simulation of biogas diffusion from the lumen to the bulk liquid. For example, **Figure 4.2** shows model output with the baseline parameters. **Figure 4.2a** shows that most of the CO_2 was transferred within the first 40 mm of the lumen, whereas **Figure 4.2b** shows that CH_4 continued to diffuse along the length of the fiber. The average CO_2 and CH_4 concentrations at the lumen effluent were 0.8 and 200 mg/L, respectively. These values mean that the simulated biogas was enriched to >99% CH_4, meeting the purity requirements for exiting the fibers for Deliverable 4.2 and Milestone 4.2. In addition, the carbon transfer efficiency (CTE) was virtually 100%. For comparison, experimental results generally achieved > 98% CTE and lumen CH_4 effluent concentrations between 85-90%. The lower effluent CH_4 concentrations were largely due to counter diffusion of O_2 from the bulk liquid through the membrane and into the lumen; counter diffusion of O_2 was not included in these initial COMSOL simulations, but is included in simulations described below.

Table 4.2. Baseline diffusion constants for CH_4, CO_2, and O_2 in the different sections

m^2/s	CO_2	CH_4	O_2	Source
Lumen	$1.03x10^{-5}$	$1.03x10^{-5}$	$1.03x10^{-5}$	Roberts (1972)
Inner membrane layer	$1.03x10^{-5}$	$1.03x10^{-5}$	$1.03x10^{-5}$	Roberts (1972)
Middle membrane layer*	$1.4x10^{-11}$	$6.07x10^{-13}$	10^{-11} †	This work
Outer membrane layer	$1.67x10^{-9}$	$1.62x10^{-9}$	$5x10^{-9}$	Engineering ToolBox (2008)
Bulk liquid	$1.67x10^{-9}$	$1.62x10^{-9}$	$5x10^{-9}$	Engineering ToolBox (2008)

*experimental value †assumed value

The results in **Figure 4.2** also suggest that the length of the fiber could be reduced significantly without affecting the amount of CO_2 supplied to the bulk liquid while also minimizing CH_4 diffusion to the bulk liquid. To evaluate this interpretation, we ran the model with a fiber length

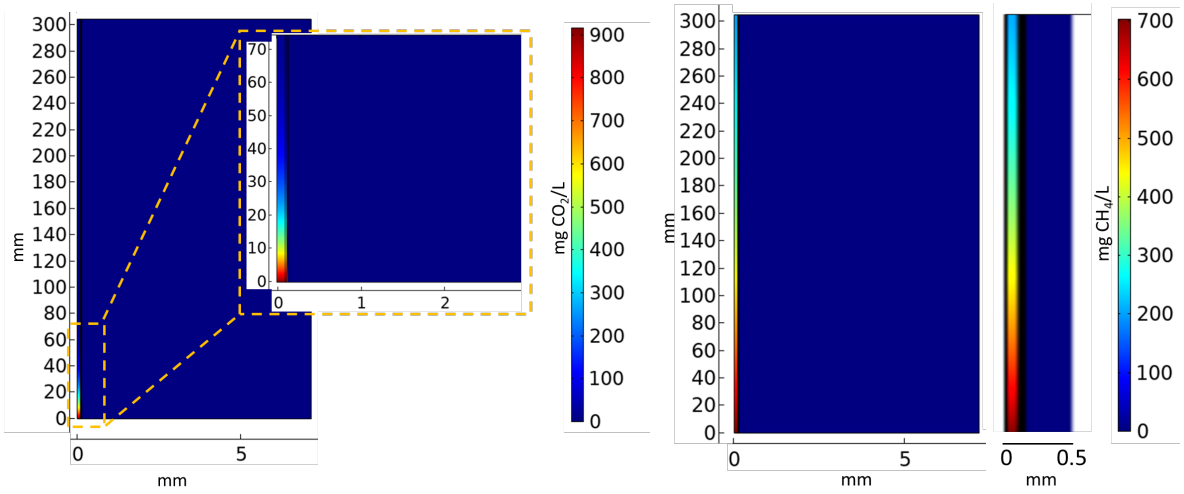

Figure 4.2. System performance based on the baseline parameter values and membrane length of 305 mm: (a) CO_2 concentrations and (b) CH_4 concentrations.

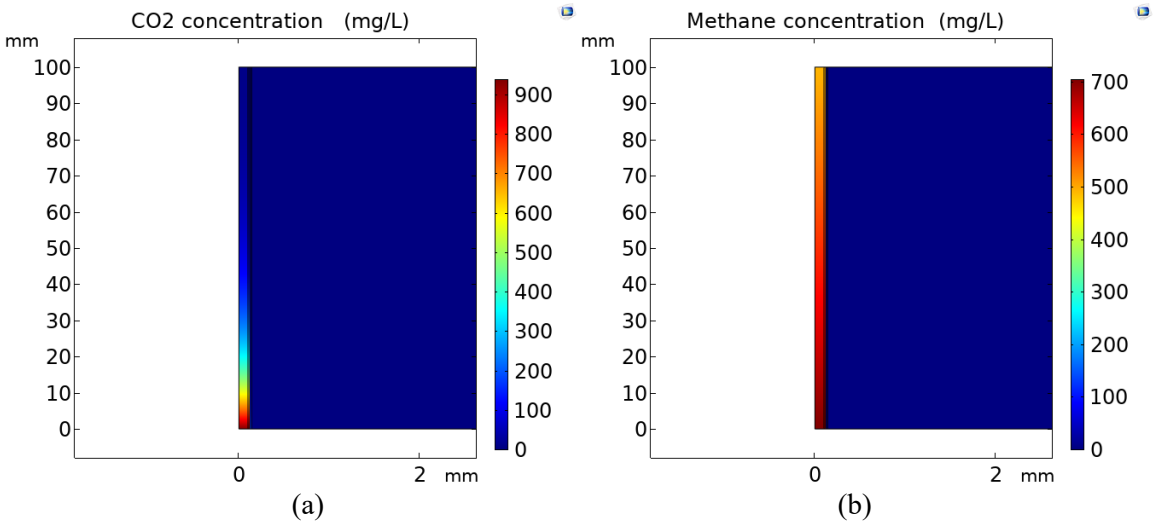

Figure 4.3. System performance based on the baseline parameter values and a membrane length of 100 mm. (a) CO_2 and (b) CH_4 concentrations.

of 100 mm (versus 305 mm), with the results shown in **Figure 4.3**. The average CO_2 concentration exiting the lumen was 9.5 mg/L, which is about 10-fold higher than the 305-mm long fibers, but the CO_2 loss was still < 1%. The effluent CH_4 concentration was 493 mg/L, which is corresponds to 98% CH_4. Thus, reducing the length could allow for reducing cost while still meeting the exiting CH_4-gas purity goal and without jeopardizing the CO_2 CTE. More generally, the results in **Figures 4.2** and **4.3** illustrate the trade-offs between CH_4 purity and CO_2 CTE.

Since O_2 can be produced by microalgae at concentrations that exceed typical dissolved-oxygen (DO) saturation levels in water, the model was modified to include counter diffusion of O_2 into the lumen. **Figure 4.4** illustrates how effluent biogas composition changed with increasing bulk O_2 concentrations based the values for O_2 diffusion listed in **Table 4.2** and a fiber length of 305 mm. In this scenario, the bulk-liquid flow rate parallel to the membrane was so fast that all of the fibers were exposed to the same (influent) O_2 concentration. **Figure 4.4** shows that an increasing DO concentration in the bulk liquid led to more O_2 in the gas exiting the lumen: up to 6.7% for a bulk-liquid with a DO of 32 mg/L. The higher O_2 in the lumen effluent reduced the total concentration of CH_4 in the effluent from 99% with no DO to 92.5% at a DO concentration of 32 mg/L. This change compares well to O_2 concentrations observed during bench and outdoor experiments, where CH_4 purity from the lumen effluent was 85-90%. The results in **Figure 4.4** underscore the value of reducing the amount of O_2 in the bulk liquid. They also reiterate the importance of empirically determining diffusion constants for all the components in the gas, membrane, and liquid phase.

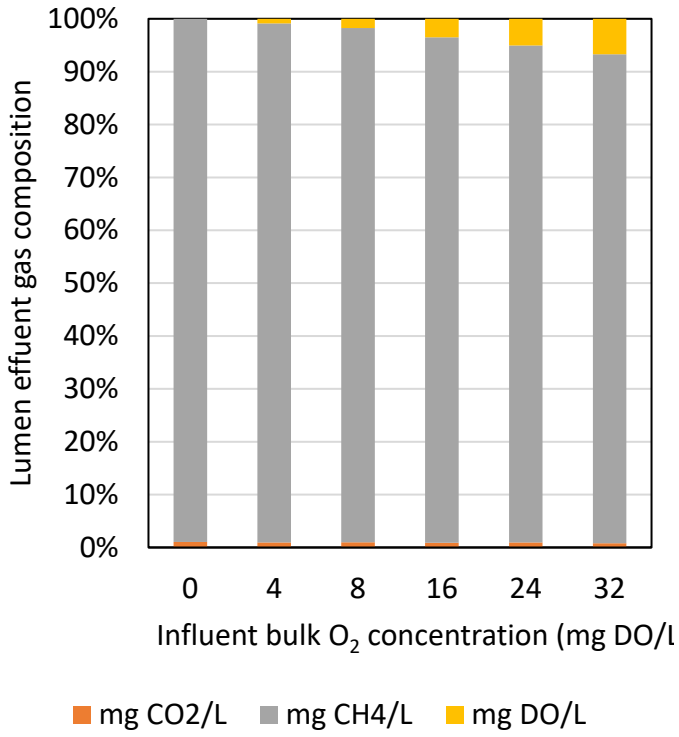

Figure 4.4. Biogas composition exiting the lumen (on a mass-percentage basis) with different bulk liquid DO concentrations.

The COMSOL model also was used to explore mass transfer using updated mass transfer coefficients, k_L, that we obtained from abiotic CH_4- and CO_2-transfer experiments; the coefficients are summarized in **Table 4.3**. For these experiments, the membrane bundles consisted of 32 membranes, each 15-cm long. The membranes were supplied a biogas mixture of 65% CH_4 and 35% CO_2 at 5 sccm, 10 psig (24.5 psia), and 23 °C. This flow rate was about 6.5 cm^3/min for ambient temperature and pressure. The membranes were submerged in a reactor filled with 23°C water at pH 10. The reactor was operated for 135 minutes. Other parameters are summarized in **Table 4.4**. The CO_2 fluxes shown in **Table 4.3** were obtained from TOC measurement (the net inorganic carbon increase normalized by the duration of tests); they are slightly lower than the values (1111 ± 58 g/m_2/d (~15 cm fiber length) vs 1068 ± 151 g/m_2/d (~30 cm fiber length)) obtained from the pH method using the same conditions (Figure 2.3). The TOC measurement was established as the better method for assessing the mass balances, as is documented in the section on CH_4 Loss Validation and Figure 2.4. Some discrepancy in flux is expected to occur between the two approaches and between two different bundles. The variation between two measurements was less than 15%, which is within the expected range (Shesh et. al, 2019). Thus, the k_L values in **Table 4.3** have a sound experimental basis.

Table 4.3. Calculated mass transfer coefficients and product from the effluent of the lumen

	Mass transfer coefficient, k_L (m/min)	Gas composition exiting lumen (%)	Mass flux into liquid ($g/m^2/d$)
Experiment 1:			
CH_4	$4.13x10^{-4}$	82	63
CO_2	$3.97x10^{-4}$ - $4.34x10^{-4}$	18	862
Experiment 2:			
CH_4	$3.71x10^{-4}$	81	44
CO_2	$3.83x10^{-4}$ - $3.94x10^{-3}$	19	820

Unless otherwise specified, the diffusion coefficient for gas i through the membrane was calculated as

$$D = k_L \delta_{mem} \quad \text{(Eqn. 1)}$$

where δ_{mem} is the thickness of the membrane wall; all values are summarized in **Table 4.4**.

The COMSOL model was formulated and executed with the mass-transfer coefficients for Experiment 1 (**Table 4.3**) and with the other parameters summarized in **Table 4.4**. Because COMSOL is unable to simulate mixing in the bulk liquid, we modeled the bulk liquid as a continuous flow of bulk liquid running parallel to the membranes at a flow rate of 500 mL/min, which minimized the mass transfer resistance from the outer layer of the membrane to the bulk liquid.

Table 4.4. Parameters for COMSOL modeling

Parameter	Units	General	Chemical specific values		Source
			CH_4	CO_2	
Lumen operational parameters					
Lumen radius	µm	100			Mitsubishi
Fiber length	cm	15			Experiments
Effluent flow rate	sccm	6.5			Experiments
Inlet and outlet pressure	psia	24.4			Experiments
Influent gas composition			65%	35%	Experiments
Diffusion coefficients in gas for the lumen	m^2/s		$1.06x10^{-5}$	$1.06x10^{-5}$	Literature
Membrane operational parameters					
Membrane thickness	µm	40.8			Mitsubishi
Mass transfer coefficient through the membrane	m/min		$7.58x10^{-7}$	$1.75x10^{-5}$	Experiments
Bulk liquid operational parameters					
Flow rate	mL/min	500			Model only
Distance between outer membrane wall and vessel wall	cm	4.5			Experiments
Pressure	psia	14.7			Experiments
Initial concentrations	mg/L		0	0	Experiments
Diffusion coefficient in water for the bulk liquid	m^2/s		$1.62x10^{-9}$	$1.67x10^{-9}$	Literature

Using the experimental mass-transfer coefficients (**Table 4.3**), we explored 7 scenarios, summarized in **Table 4.5**. The baseline scenario is consistent with the conditions in **Table 4.4**. Scenario 2 slightly increases the mass-transfer coefficient of CO_2 to match that of CH_4 in Scenario 1. For scenario 3, the baseline mass transfer coefficients were increased 10-fold. For scenarios 4 and 5, the CH_4 mass transfer coefficient was decreased, while the CO_2 coefficient was held constant. For scenarios 6 and 7, the CO_2 mass transfer coefficient was increased, while the CH_4 coefficient is 10 times lower than the baseline.

Figure 4.5 summarizes the result and shows that, when the mass transfer coefficient for CH_4 was held at the experimental (baseline) value or an order of magnitude higher than baseline (scenarios 1−3), the model under-estimated the CH_4 composition of the gas exiting the lumen by 1–9%: 70–76% CH_4, versus 77–85% CH_4 in the outdoor experimental system. The model outputs also under-estimated the average maximum CO_2 flux into the bulk liquid by 4 times: 198–384 g CO_2/m^2-d versus 820–862 g CO_2/m^2-d in the experiments. Scenarios 4−7 show that decreasing the mass transfer coefficient by 10- to 100-fold for CH_4 resulted in the flux being consistent with experiment values (decreased to 16–149 g CH_4/m^2-d in the model versus 44–63 g CH_4/m^2-d in experiments). To achieve CO_2 fluxes comparable to experimental values, the CO_2 mass-transfer coefficients had to be increased by 10- to 100-fold (scenarios 6 and 7). Scenario 7 resulted in values similar to experimental values – including observed mass fluxes and lumen exit concentrations (82% CH_4 experimental vs. 84% model values).

In summary, the CO_2 mass-transfer coefficient had to be increased to match simulation results with experimental results. The main problem with the COMSOL simulations is that COMSOL was not able to represent the chemical speciation of CO_2 to HCO_3^- or CO_3^{2-} in the bulk liquid. Speciation to HCO_3^- or CO_3^{2-} provides additional driving force for CO_2 diffusion into the liquid and increase CO_2 mass transfer to the bulk liquid and depletion of CO_2 in the lumen's exit gas. Increasing the CO_2 mass-transfer coefficient was a means to "get around" the fundamental limitation of COMSOL, and it supports the inherent importance of including chemical speciation in the liquid.

Table 4.5. Summary of modeling scenarios for different CH_4 and CO_2 mass transfer coefficient values

		Mass transfer coefficient ($g/m^2/d$)	
Scenario	**Description**	**CH_4**	**CO_2**
1	Baseline scenario	$4.13x10^{-4}$	$3.97x10^{-4}$
2	Diffusion coefficient in the lumen and membrane are the same	$4.13x10^{-4}$	$4.13x10^{-4}$
3	10x larger mass transfer coefficient	$4.13x10^{-3}$	$4.34x10^{-3}$
4	10x smaller CH_4 mass transfer coefficient	$4.13x10^{-5}$	$4.34x10^{-4}$
5	100x smaller CH_4 mass transfer coefficient	$4.13x10^{-6}$	$4.34x10^{-4}$
6	10x smaller CH_4 and 10x larger CO_2 mass transfer coefficient	$4.13x10^{-5}$	$4.34x10^{-3}$
7	10x smaller CH_4 and 100x larger CO_2 mass transfer coefficient	$4.13x10^{-5}$	$4.34x10^{-2}$

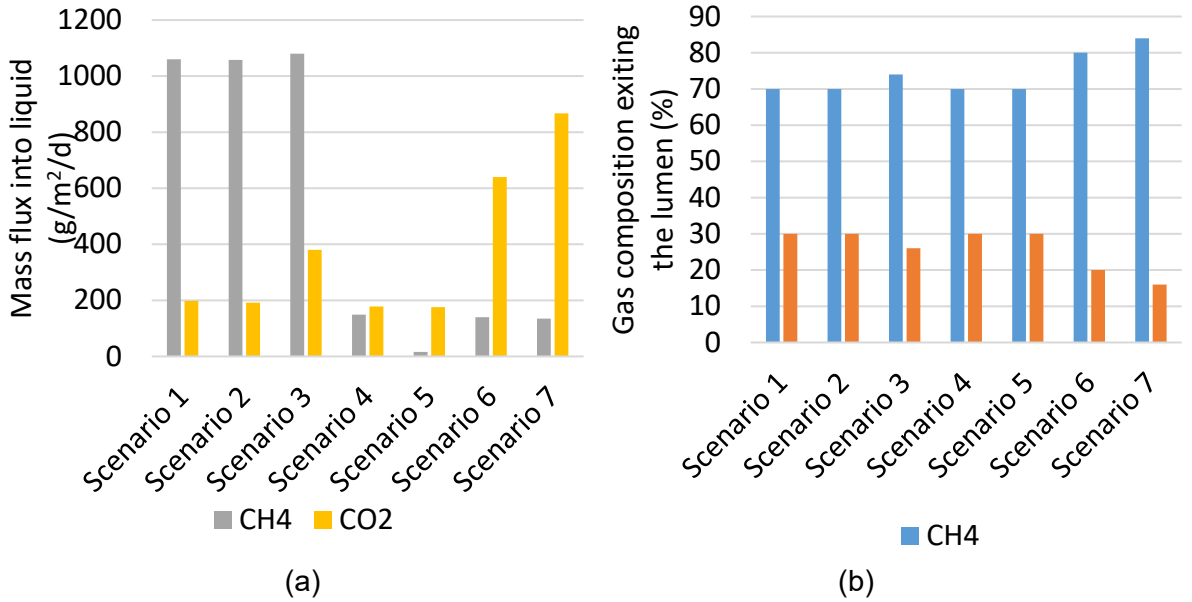

Figure 4.5. Gas composition exiting the lumen and mass flux into the liquid for CH_4 and CO_2 in the scenarios summarized in Table 4.5.

Based on in-depth discussions with COMSOL technical experts, we realized that we could not execute a membrane model that couples mass transfer with chemical speciation in the bulk liquid. Therefore, we tried to modify the MATLAB program MYANODE to predict CO_2 transfer into a CSTR in which chemical speciation occurs (Young, 2018). MYANODE was used originally to describe chemical speciation and diffusive transport in microbial electrochemical cells. The platform has much of the code needed to describe the MC system: diffusion through media, chemical speciation and pH computation, diffusion into a bulk liquid, a bulk liquid that can be described as a continuously stirred tank or a well-mixed batch reactor, and gas-liquid phase transfer. However, the modified MYANODE program did not reliably converge; when it did converge, it took untenably long times to reach convergence. The convergence problem can be attributed to the pH calculations, which are notoriously time-consuming and unstable. Therefore, we were unable to link chemical speciation to MC gas transfer. Given the importance of speciation, developing a model that includes speciation and mass-transfer kinetics will be highly valuable future work. This might be accomplished using the MYANODE format by fixing the pH in the bulk liquid, as is done in practice using MC.

Key Outcomes:

- The COMSOL model provided valuable insights into the tradeoffs among membrane length, CH_4 enrichment, and cost factors. For instance, a significantly shorter membrane length (100 cm vs 305 cm) could be used to achieve similar CH_4 enrichment (98% vs 99%), while lowering capital costs.
- COMSOL modeling also identified the challenge of O_2 diffusion into the membrane lumen, which reduces CH_4 enrichment. As the influx of O_2 increased with bulk-liquid DO concentration, the modeling points out the value of O_2 degassing in the bulk liquid.

- COMSOL was unable to model transport phenomena coupled with complex chemical speciation routines dependent upon pH, and our attempt to modify MYANODE did not succeed due to it taking too long to converge.
- Results using COMSOL without chemical speciation identified the value of including speciation is future modeling, since the COMSOL model underestimated CO_2 mass flux by four-fold and, consequently, underestimated CH_4 composition in the effluent stream.
- Underestimated CO_2 flux using realistic mass-transfer coefficient was due to lack of chemical speciation, which adds additional driving force due to CO_2 gas being converted to CO_3^{2-} at the experimental pH. Applying the MYANODE format with a fixed pH is a promising path forward.

Task 5 – Design, manufacture and installation of membrane modules for use in small-scale outdoor cultivation at Arizona Center for Algae Technology and Innovation (AzCATI)

The purpose of Task 5 was to develop and install MC modules into the 4-m^2 raceways at AzCATI, complete with mass flow and gas sensors to develop a carbon mass balance on the system. During this task, a custom-built gas analyzer with data-logging system was designed to track influent and effluent gas flow for ponds using membrane carbonation (**Figure 5.1A**) and sparged influent flow (**Figure 5.1B**). The gas analyzers for MC raceways used mass flow meters and CO_2, CH_4, and O_2 sensors to quantify the gas composition going into and out of the membrane modules. All sensors and mass flow meters for the systems were connected to a central data logging unit with a logging frequency of every 2 minutes to provide high resolution data. **Figure 5.2** shows the installation of these boxes on the elevated raceways on the east side of the AzCATI field site. To ensure gas composition, custom gas-cylinders were ordered and placed next to the raceways with stainless steel tubing connecting to the gas analyzer boxes to minimize gas diffusion in the lines. All plastic tubing were fluorinated ethylene propylene (FEP) tubing, which provides extremely low gas diffusion and high chemical/UV resistance.

This project required the manufacturing of several MC modules of different sizes. To improve the consistency of performance between the different modules, a protocol was setup to minimize discrepancy and loss of usable surface area (**Figure 5.3**). The protocol required the use silicon molds and multiple epoxies with different viscosities to ensure a gas tight seal. One of the main failures observed during the project was a softening of the epoxies at the higher temperatures experienced during the summer months. To overcome this and for future projects, it is imperative to use epoxies with a glass transition temperature greater than 50°C.

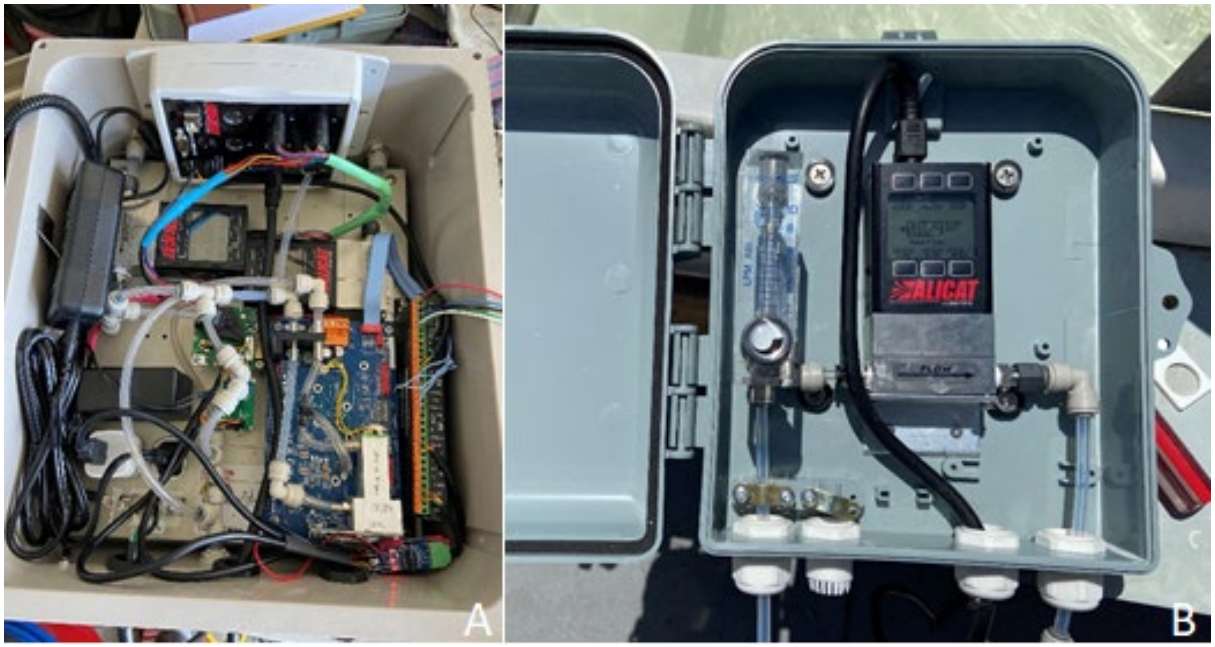

Figure 5.1. A) Inside of a gas analyzer box designed for tracking mass flow, CO_2, O_2, and CH_4 going through MC system during cultivation. B) Mass flow totalizer system for tracking total flow and instantaneous flow in the sparging raceways serving as controls.

Figure 5.2. A) Gas regulator installation next to raceways. B) Installation of mass flow meter box on a sparging raceway. C) Mass flow meter and gas analyzer box on raceway 1. D) Primary data logger box and mass flow meter and gas analyzers on raceway 2. Note that raceway 3 has an identical box to that on raceway 1.

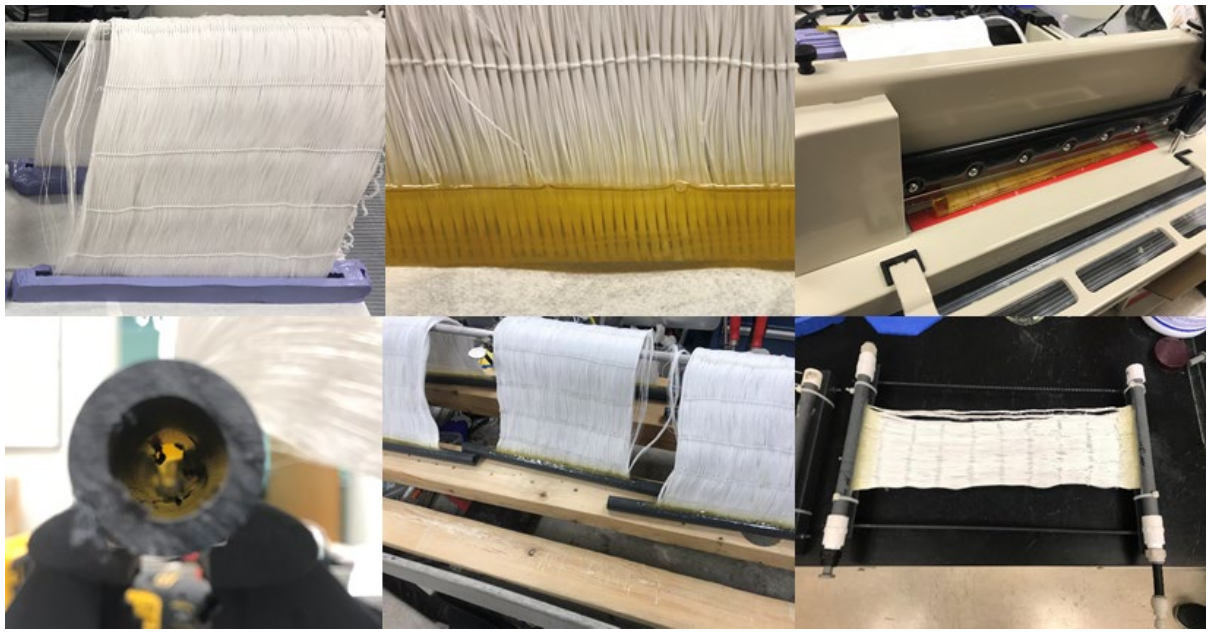

Figure 5.3. Photographic visual representation of the different steps in manufacturing the membrane modules.

Key Outcomes: The gas analyzer instrumentation was the first-of-its-kind to be deployed at AzCATI and has provided the most complete view of gas transfer into the outdoor algal raceways at AzCATI. The instrumentation was crucial in being able to quantify the carbon transfer and carbon utilization efficiency in the raceways. Throughout the project, a total of 10 small and 8 large membrane carbonation modules were manufactured using the described protocol with a relatively high success rate. Further increasing the accuracy and repeatability of manufacturing these modules was beyond this scope of the proposed research and would require a dedicated facility for manufacturing membranes with the proper equipment.

Task 6 – Initial outdoor trials without H_2S - Three outdoor cultivation trials using membranes over multiple seasons

Cultivation in the outdoor 4-m^2 raceways occurred during two trials, from August 30th to October 12th, 2020, and from February 17th to April 8th, 2021. Due to culture crashes at AzCATI during the summer of 2020, the first trial was delayed by 2 months. To minimize disruption to the rest of the project, the second winter trial scheduled for November and December was removed, as it was close to the end of the first trial and would provide similar results to those of the trial in February. In each trial, the cultures were grown with synthetic flue gas for greater than 3 weeks and then switched to synthetic biogas. This task addresses Milestone 6.1.1 and 7.1.1. Due to supply-chain delays, we were unable to acquire synthetic biogas with H_2S for the 4-m^2 trial in Task 7. Therefore, the second trial from February through April 2021 is included with Task 6. The composition for each can be found in **Table 6.1**. In the first set of experiments, cultivation was accomplished using *Picochlorum celery* (Pico). This strain was used in place of *Scenedesmus obliquus* UTEX 393 due to contamination issues on the AzCATI field site that prevented long-term cultivation during the hot summer months. To track the carbon balance in the cultures, samples were taken on weekdays for carbon analysis, ammonia concentration, and alkalinity.

Table 6.1. Synthetic gas composition used in Task 6.

Gas Component	Flue Gas	Biogas
CO_2	14	35
N_2	81	-
O_2	5	-
CH_4		65

Cultivation with flue gas was completed from August 31st to September 21st and from September 22nd to October 12th, 2021 with biogas. The data described in this report focus on detailed sample analysis from the mornings of Sept 14th to Sept 21st for flue gas and October 6th to October 12th for biogas. A key change in cultivation was the pH setpoint of 7.75, which is above the ideal growing pH of 7 for Pico and what is traditionally used for SOT trials. The increased pH was chosen to reduce CO_2 off-gassing from the surface of the raceways. **Table 6.2** shows the CTEs, CUEs, and biomass productivities for the flue gas and biogas trials. The reduced biomass productivity target for biogas was due to growth occurring during late September and early October, which has reduced growth rates compared to growth in early September.

Table 6.2. Results for key performance targets CTE, CUE, and productivity for Fall 2020 experiments at AzCATI

Gas	Metric	Target	Experimental
Flue Gas	CTE	60%	90 ± 6%
	CUE	50%	55 ± 1%
	Productivity	> 5% increase from 13.3 g/m^2/d	16.1 g/m^2/d
Biogas	CTE	60%	92 ± 9%
	CUE	50%	68 ± 16%
	productivity	> 5% increase from 10.0 g/m^2/d	13.5 g/m^2/d
	CH_4 purity	80%	83-95%

[a] Productivity comparison is against SOT 2016 seasonal measurements.

The second set of experiments, shown in **Table 6.3**, was conducted from February 17th to March 10th and March 12th to April 8th, 2021, on synthetic flue gas and biogas, respectively. As these experiments were conducted during the late winter, early spring months, *Monoraphidium minutum* 26B-AM was the cultivated species. As the Spring 2021 experiment was conducted with a freshwater alga grown at 5 ppt salt, the CTE for flue gas was reduced and CUE for the cultures was lower. However, the Fall 2020 experiment was conducted with a saltwater species grown at 32 ppt salt, which had a measurable increase on the CTE of the cultures and the retention of CO_2 in the culture media. In all experiments, the CUE was significantly lower than CTE and is attributed to the loss of CO_2 to atmosphere from off-gassing. This is extremely problematic in 4-m^2 raceways, as the paddlewheel is disproportionately large compared to commercial scale raceways. This increases the net off-gassing, as paddlewheels provide a high level of mixing and aeration that increases the interaction of the culture liquid with the atmosphere. This underscores the importance of finding approaches with higher pH setpoints in addition to having high transfer efficiency. In both the Fall 2020 and Spring 2021 cultivation trials, the pH setpoint was 7.75, while the approximate equilibrium pH with the atmosphere was closer to 8.3. This created a large CO_2 surplus in the culture media to help drive photosynthesis. However, this also created a driving force with the atmosphere that causes the CO_2 to be off-gassed. The pH setpoint of 7.75 increased the CUE of the Pico cultures to close to >55%, while growth at a pH setpoint of 7 had a CUE <20%. Future work is needed to better understand the trade-offs between pH and CUE to optimize and improve the feasibility of algal cultivation.

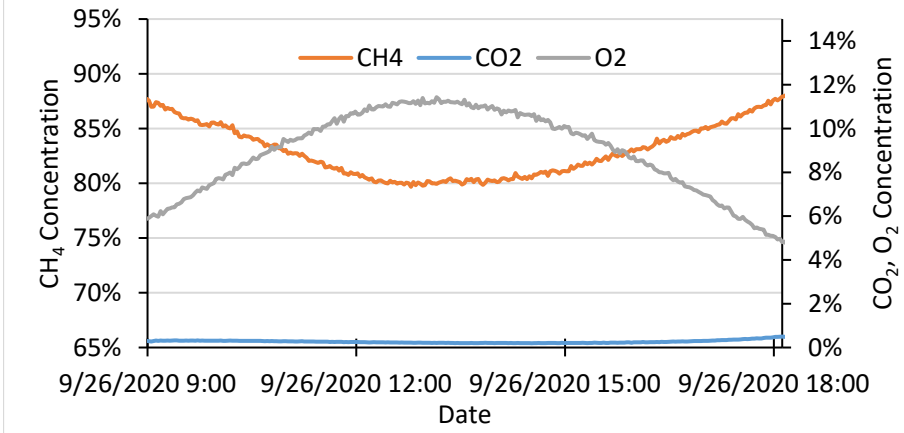

Figure 6.1. Example of diurnal variation in effluent gas composition from MC modules.

For experiments that utilized biogas, the effluent biogas quality

Table 6.3. Results for key performance targets CTE, CUE, and productivity for Spring 2021 experiments.

Gas	Metric	Target	Experimental
Flue Gas	CTE	75%	83 ± 4 ± %
	CUE	65%	38 ± 2± %
	Productivity	> 5% increase from 7.0 g/m^2/d	8.9 g/m^2/d
Biogas	CTE	75%	90 ± 4± %
	CUE	65%	57 ± 5± %
	productivity	> 5% increase from 11.0 g/m^2/d	12.2 g/m^2/d
	CH_4 purity	80%	83-95%

[a] Productivity comparison is against SOT 2016 seasonal measurements

depended on the time of day, as shown in **Figure 6.1**. However, the highest CH_4 content consistently occurred during the morning sun. This is attributed to two factors. **1)** The raceway temperature was the lowest in the morning, which increased gas solubility, allowing for additional CO_2 to be removed from the membranes. **2)** Dissolved oxygen over-saturation was at the lowest levels in the morning, which reduced the amount of O_2 counter-diffusing into the membrane lumen. The largest change from abiotic results (Task 2) is the significant O_2 diffusion into the membrane, which reached up to 15% O_2. These results concur with the indoor biological results found in Task 3 and suggest that different membranes will be needed to better separate and purify the biogas.

When completing the mass balance on the membranes, it became apparent that the mass of CH_4 in the effluent was less than that entering the fiber. This is attributed to CH_4 crossing the membrane wall and dissolving into the culture media. An worst-case oversimplification is that all CH_4 that entered the culture medium was lost to the atmosphere. A more detailed mass balance on CH_4 was completed for the indoor experiments (**Task 3**) and showed that a portion of the methane may be consumed by microorganisms in the medium. In the outdoor trials, the CH_4 loss ranged from 5-50%, depending operating pressure, temperature, fiber age, membrane configuration, and leaks. Operating conditions with lower pressures (10-15 psig) and newer fibers without leaks had CH_4 loss between 5 and 15%. When fibers developed leaks and/or were operated at higher pressures (20-30 psig), the CH_4 loss was 20-50%. In a preliminary LCA, it was identified that a leak rate of $\geq$ 0.28% would make the GHG emissions from the process exceed those needed for the renewable fuel standards. Thus, further work is needed to identify methods to reduce and/or capture the CH_4 that is crossing the membrane wall.

Key Outcomes: We demonstrated evidence of meeting Milestone 6.1.1 [Go/No-Go] and SMART Milestone 7.1.1 by cultivating with membrane carbonation delivering synthetic biogas and flue gas, each for 3 weeks with 83–92% carbon delivery (transfer) efficiency, which is $\geq$ the required 75%; 54–79% CUE, which partly exceeds the required $\geq$ 65% as required; a $\geq$ 5% increase over SOT productivity; and CH_4 purity of 80–95% from biogas, which is the required $\geq$ 80%.

Task 7 – Outdoor cultivation trials evaluating H_2S in membranes

Due to supply-chain restrictions, the original goal of using synthetic biogas with H_2S in the 4-m^2 raceways in subtask 7.1 became the second trial in Task 6, which also shifted Milestone 7.1.1 into task 6. Task 7 now exclusively involves the experimental trial with real biogas set at the City of Mesa's Northwest Water Reclamation Plant. Because of vendor delays, which lead to shorter trials at AzCATI, milestone 8.2.1, utilized the data from the onsite trial using real biogas.

Figure 7.1 shows the installation of the three 25-m^2 raceways at the Northwest Wastewater Reclamation Plant, which occurred in September 2021. Raw biogas was plumbed to each raceway, with gas sensors and flow controllers to track MC module performance. Once the biogas exited the MC modules and gas sensors, the upgraded biogas was dried and passed through an activated carbon filter designed to prevent the release of H_2S.

Figure 7.1. Installation of the three 25-m^2 raceways at the City of Mesa Northwest Water Reclamation Plant.

Each pond had 1 or 2 MC modules installed just after the paddlewheel (**Figure 7.2**). Each module was designed in Task 5 and contains ~3-m^2 of fiber surface area and ~11,000 individual fibers. In ponds with 2 modules, they were run in parallel. To accommodate the large surface area, 2 layers of sheets were placed into the mold. This approach had shown to be effective in the Fall 2020 experiments in Task 6;

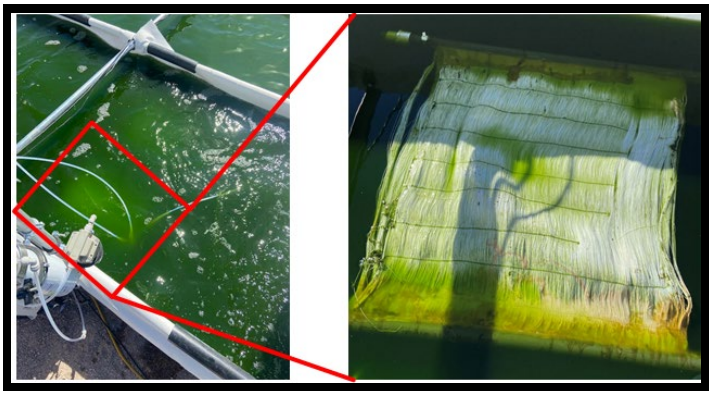

Figure 7.2. MC module installment in each raceway. Each module contains 3-m^2 of membrane surface area.

however, in the large raceways, this led to an area for biofilm formation and an area for predators to collect.

Figure 7.3. Raceways started to develop a diverse ecological profile not seen at the smaller scales.

Due to the use of reclaimed water and not altering the salinity to 5 ppt, as was done in Task 6, the culture developed ecological diversity that did not form at the AzCATI facility (**Figure 7.3**). Identified organisms include water scavenging beetles, dragon fly nymphs, snail eggs, and midge flies. If the experimentation were to continue longer, the development of the ecological community may have further diversified. **Figure 7.4** documents the entire species life cycle for the midge fly within a single pond. This has significant long-term effects on the project's final goals. As algae are the primary producer in the raceway, the development of an ecological community reduced suspended-biomass productivity and carbon utilization efficiency through algae consumption. Future research will be needed to understand the net loss of algal biomass productivity to consumption by insects.

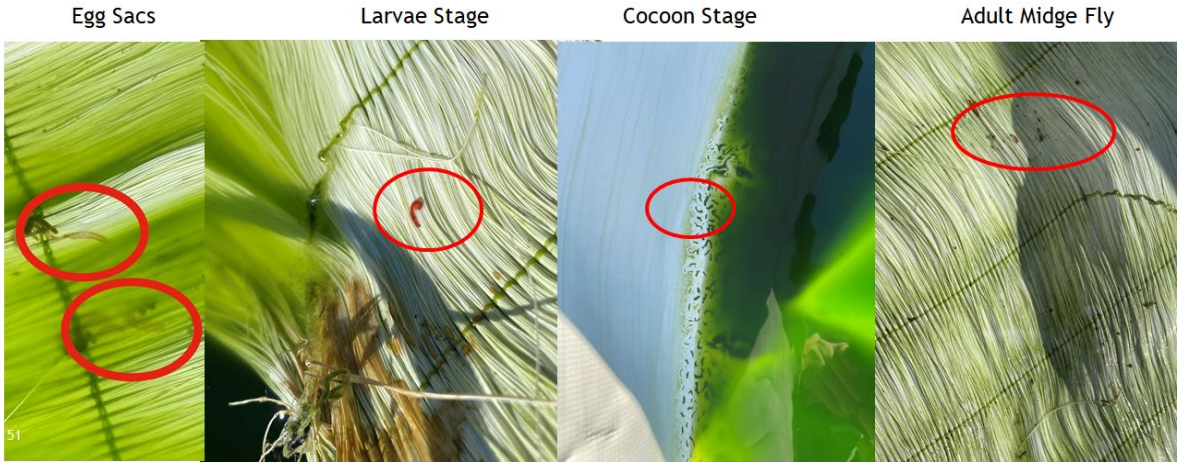

Figure 7.4. Each raceway developed a complete midge fly life cycle. This reduced the net biomass productivity through biomass consumption

In addition to the presence of insects, the lower salinity and water sourced from the wastewater treatment facility led to a diverse microbial community. One of the largest differences between Task 6 and Task 7 was the development of a biofilm on the MC modules (**Figure 7.5**). This biofilm created an additional layer of mass-transfer resistance on the membrane surface, which

reduced the ability of the membrane to transfer CO_2 into the algal culture. This resulted in a decrease in the CTE of the membranes, as shown in **Figure 7.6**, which shows the daily CTE values over the course of the entire experiment. The figure also shows the high variation in the CO_2 utilization efficiency from the biogas. This can be attributed to culture settling, biomass consumption, and heterogenous culture samples.

In addition to reducing CTE, the resistance to transferring CO_2 into the culture also meant that the concentration of CO_2 in the membranes' effluent gas was higher. Figure 7.7 shows the effluent gas composition for 2 separate days. On October 21, the membranes did not have any biofilm formation and were capable of removing most of the CO_2 from the gas. However, due to the production of O_2 from photosynthesis, O_2 diffused back into the membranes, which prevented the methane from achieving the 97% project target. On November 23rd, 2021 the membrane had a significant biofilm layer. The graph shows that, with the thick biofilm, the effluent gas was ~77%

Figure 7.5. Biofilm formation on membranes in MP2.

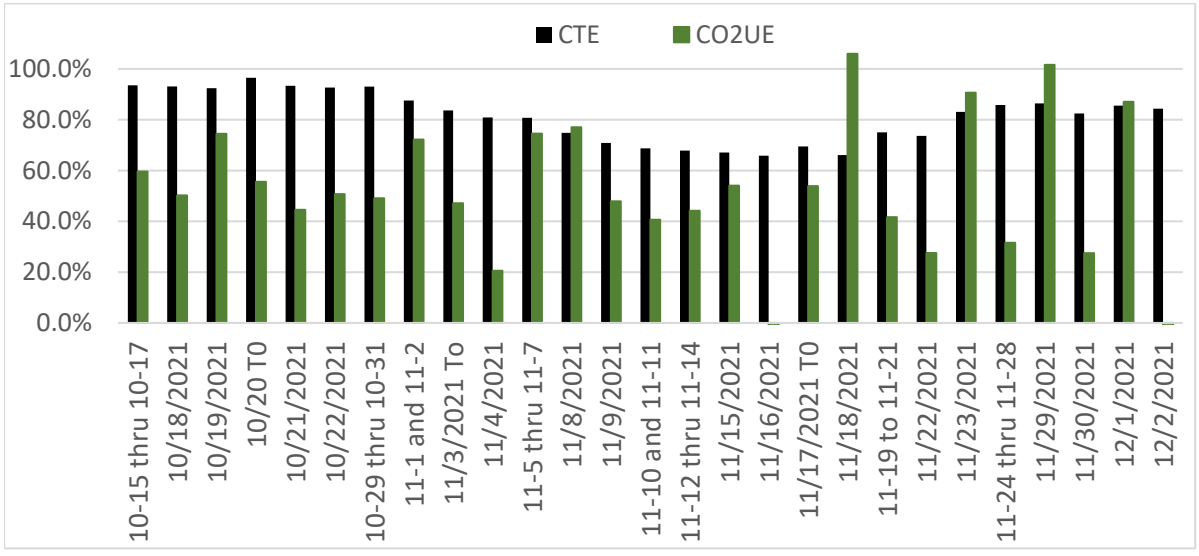

Figure 7.6. CTE (Black) and CO_2 Utilization Efficiency from biogas for experimentation at the City of Mesa's Northwest Water Reclamation Plant.

CH_4 and ~25% CO_2, but the effluent gas had less than 0.1% O_2. On November 23 in Figure 7.7, there is a distinct shift in gas composition, which occurred due to removing a majority of the biofilm. This does show that the biofilm formation can be mitigated. The impacts (negative and

positive) of the biofilm need further research to understand the tradeoffs and to understand how to mitigate problems to take advantage of benefits observed in the outdoor trials.

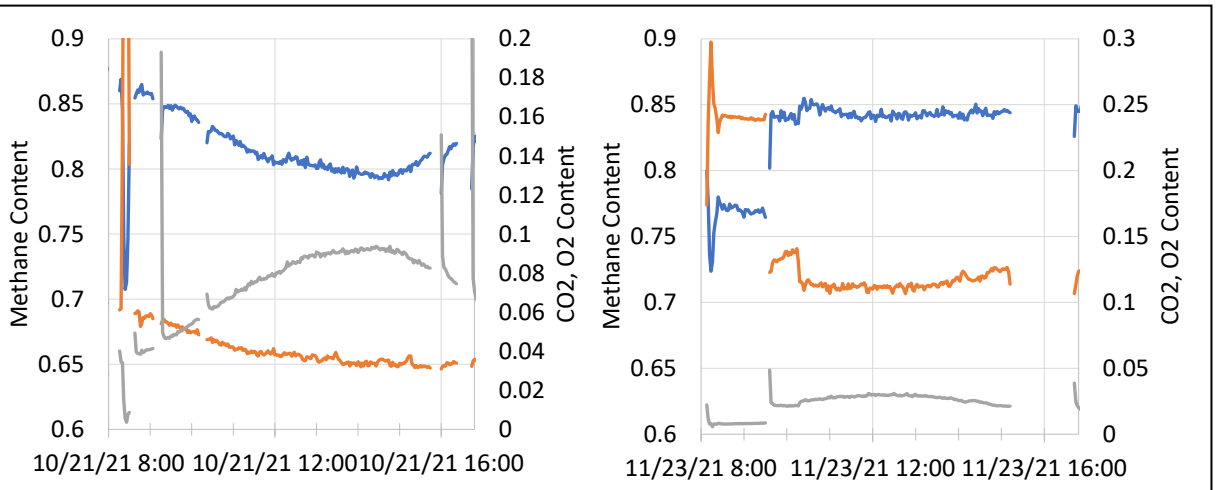

Figure 7.7. Effluent gas composition from MP2 for outdoor cultivation on two example dates. CH_4 (Blue Line), CO_2 (Orange Line), and O_2 (Gray Line) gas composition in the lumen effluent for 10/21 and 11/23 for MP2.

Microbial communities obtained from outdoor trial at the Northwest Wastewater Reclamation Plant, Mesa, AZ

Figure 7.8 shows that the microbial communities of the biomass in the bulk liquid shifted over time. The abundance of phylotypes most similar to *Methyloversatilis* increased from 8% up to 27% in pond 1 and up to 45% in pond 2. Presumably, this methylotrophic bacterium, which is

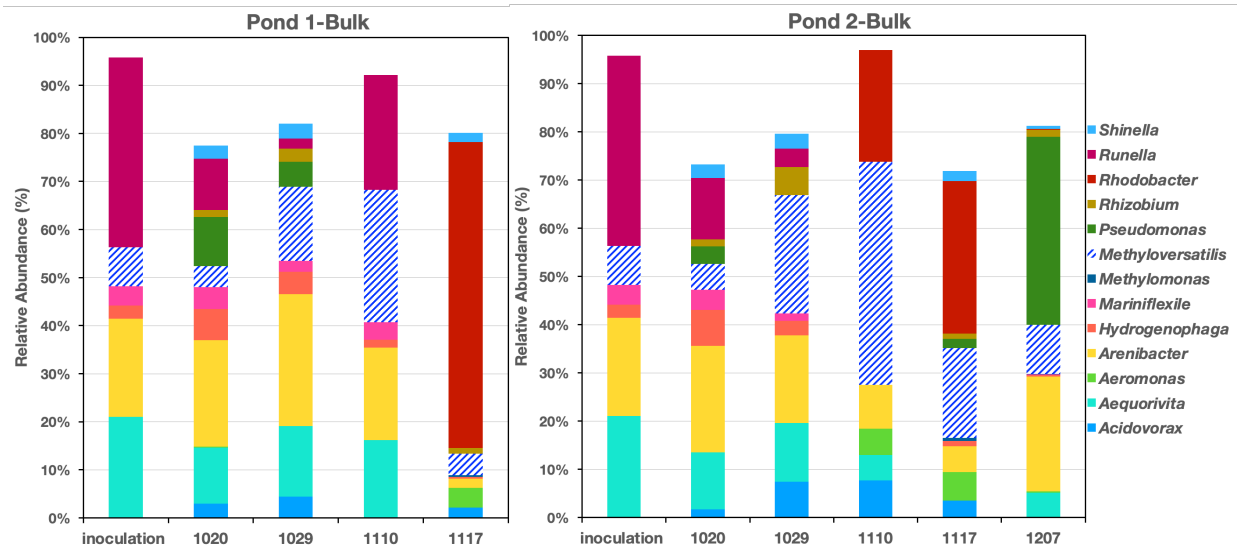

Figure 7.8. Microbial communities (at the genus level) obtained from bulk liquid of ponds from the NWRP) at Mesa, AZ. The horizontal-axis labels represent the date on which the sample was collected in October or November 2021). The percentages not shown are genera not consistently > 1%.

capable of using single-carbon compounds as sole sources of carbon and energy,[5,6] was able to utilize CH_4 coming across the membrane wall, lowering CH_4 release to the atmosphere; this explains their population increase and dominance growing over time.

Phylotypes most similar to *Arenibacter* (up to 27% abundance) and *Aequorivita* (up to 22% abundance) also were dominant parts of the microbial communities. *Arenibacter* and *Aequorivita* are aerobic bacteria and have been associated with biodegradation of hydrocarbon compounds .[7,8] Their presence may be related with biodegradation of soluble microbial products produced by microalgae in the pond. Phylotypes most similar to the heterotrophic *Runella* were present up to 40% abundance. They were carried over from the inoculum, but declined with time. Phylotypes most similar to *Rhodobacter* also were highly abundant (up to 65% in pond 1). *Rhodobacter* has an extensive range of metabolic capabilities, including the ability to do photosynthesis .[9] *Rhodobacter* suddenly bloomed in both ponds on Nov. 17, 2021. It is unclear whether the bloom was associated with the culture crash in pond 1, as crashing did not occur in pond 2. A more complete picture across multiple kingdoms may help to understand why the culture crashed, such as from a so-far-unknown invader.

Figure 7.9 shows the specific locations on the membrane module in pond 2 where biofilm samples were obtained for microbial analysis. **Figure 7.10** shows the sequencing data obtained from ponds 1 and 2 (bulk and biofilm) analyzed using principal coordinate analysis (PCoA) to visualize complex data in low-dimensional space in which points in close proximity have similar sequence compositions. The PCoA results demonstrate that the microbial communities in the biofilm were far different from the communities in the bulk liquid.

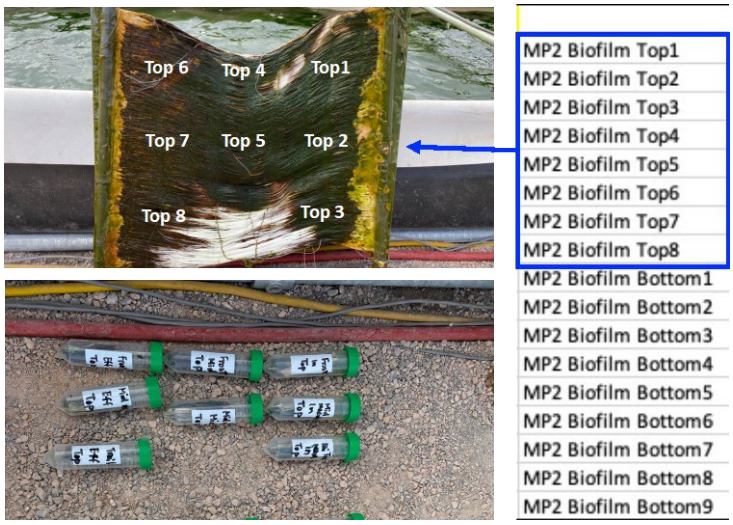

Figure 7.9. Biofilm samples were obtained from the specific locations of membrane sheet at the pond 2. Each membrane module had two sheets of membranes. The photo above shows the top layer of one sheet.

Figure 7.11 shows that microbial compositions of biofilms on the membrane sheets (in pond 2) shifted with location: gas-influent side (red dash) vs gas-effluent side (blue dash). The difference between the blue and red groups can be ascribed to the depletion of CO_2 and enrichment of CH_4 along the gas-flow path. However, the differences between biofilm and suspension were more important than whether the biofilm sample was taken from the bottom or the top of the membrane module (**Figure 7.11**).

Figure 7.12 shows the microbial communities from the biofilm samples that were obtained at the end of cultivation trial, on Nov. 17th and Dec. 7th from pond 1 and pond 2, respectively. The biofilm microbial communities from both ponds were consistent with each other. In particular, the presence of *Methyloversatilis* and *Methylomonas*, C1 utilizers ,[5,6,10] was very important. *Methyloversatilis*, which had > 25% abundance, is able to use C1 compounds as its sole electron donor and carbon source. This strongly supports that *Methyloversatilis* oxidized CH_4 transferred across the membrane wall, which likely significantly reduced CH_4 emission to the atmosphere. *Methylomonas,* which had from 2 to 7% abundance, also is a C1 utilizer that can oxidize methane and methanol.[10] Since *Methyloversatilis* can utilize a variety of C1 and multi-carbon

compounds, it may have had a competitive advantage of *Methylomonas*. Outside *Methlyloversatilis*, the microbial communities obtained from the bulk liquid (**Figure 7.8**) and biofilms (**Figure 7.12**) were generally similar, with none of the other genera gaining more than 20% abundance in the biofilms. This similarity might mean that the biomass in the bulk liquid was largely derived from detached biomass.

Shown in **Figure 7.13** are functional genes associated with C1 metabolism and identified in biofilms and bulk-liquid samples: *mcrA*-C (methyl-coenzyme M reductase subunit), *mxaL* (*mxaL* methane metabolism protein), *mxaF* (methanol dehydrogenase (cytochrome c) subunit), *mmoX* (methane monooxygenase component A alpha chain), and *pmoA-C* (methane/ammonia monooxygenase subunit).[11–14] Finding these genes confirms the potential activity for CH_4 oxidation, particularly in the biofilms, and it further supports our hypothesis that the microbial communities significantly reduce CH_4 released to the atmosphere.

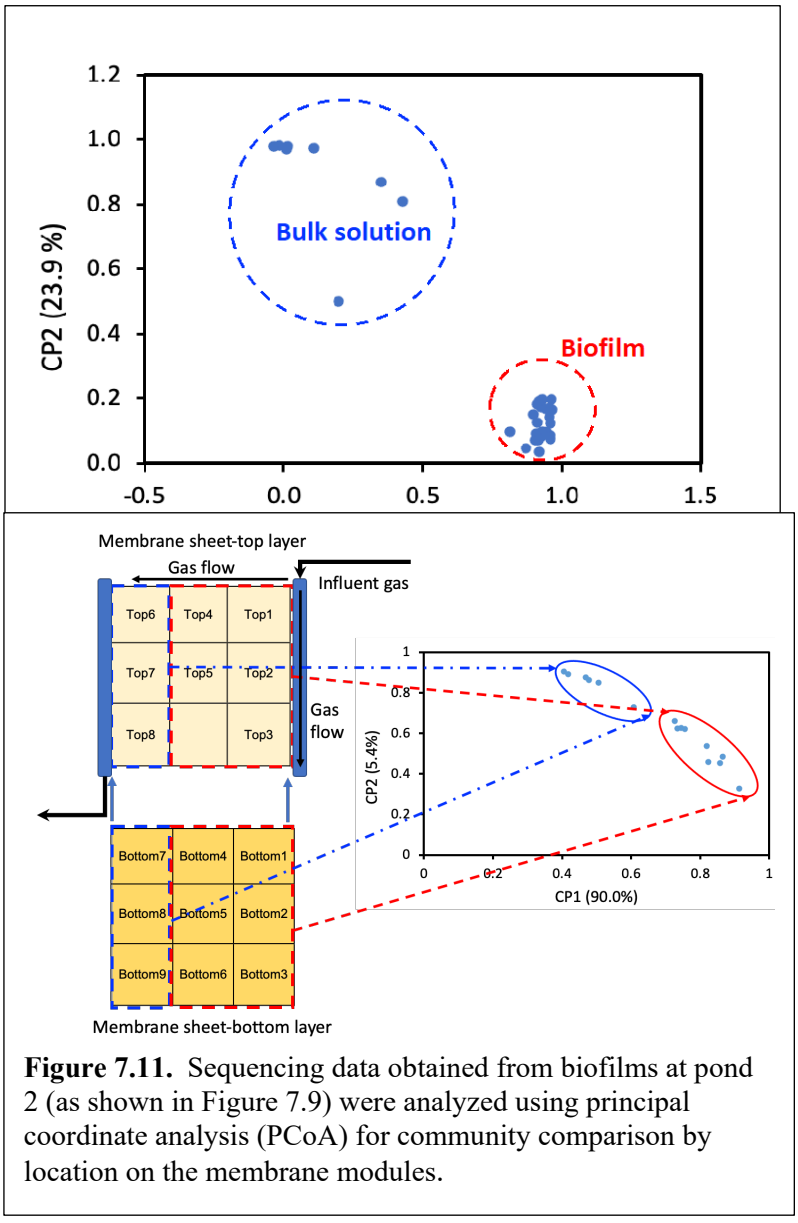

Figure 7.11. Sequencing data obtained from biofilms at pond 2 (as shown in Figure 7.9) were analyzed using principal coordinate analysis (PCoA) for community comparison by location on the membrane modules.

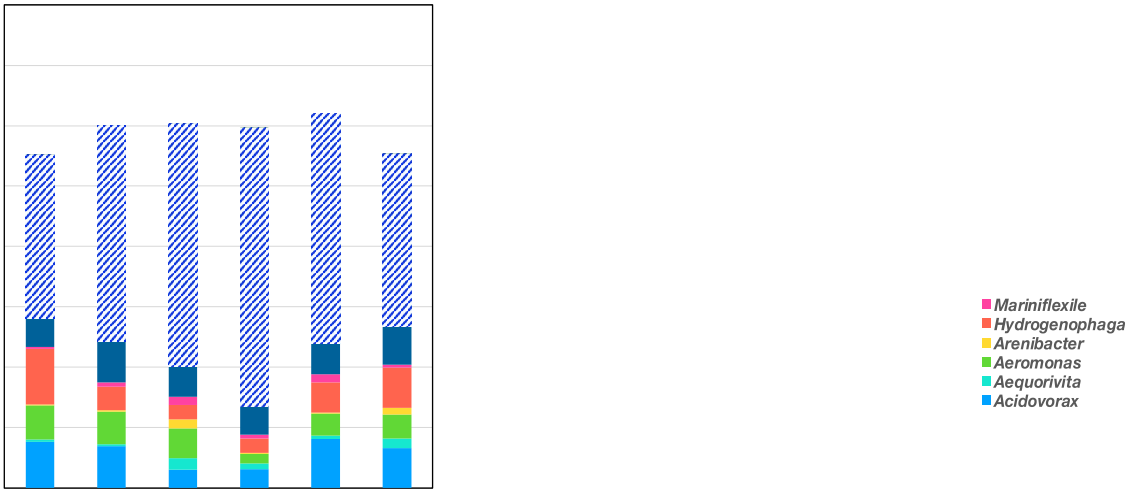

Figure 7.12. Microbial communities (at genus level) obtained from the membrane modules located at the pond 1 and pond 2. The top layer of biofilm from the pond 2 are shown here. Genera not shown had abundances consistently < 1%.

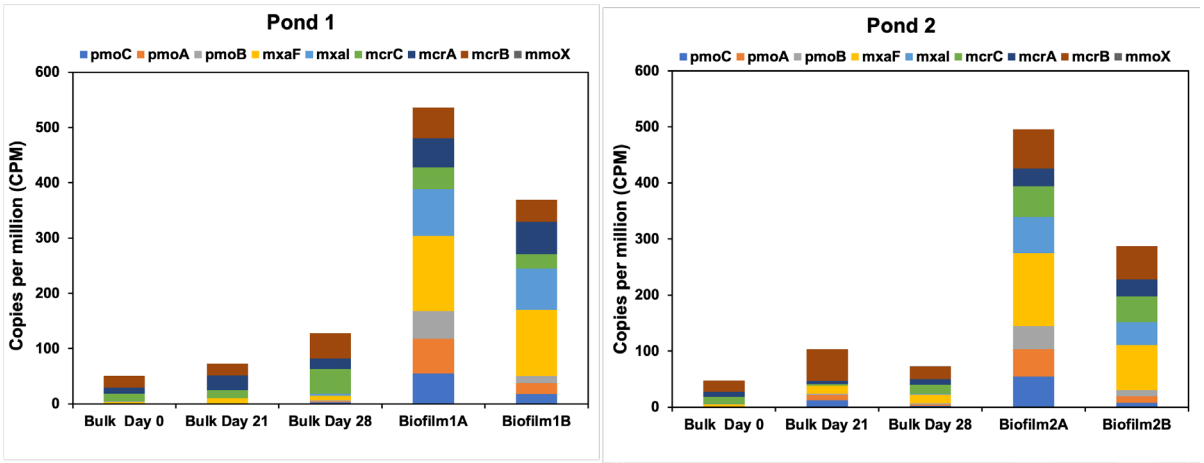

Figure 7.13 Functional genes associated with C1 metabolism identified in biofilm and bulk-liquid samples obtained from pond 1 and pond 2. The results correspond to having *Methyloversatili* and *Methylomonas* as C1 utilizers present in the biofilm and bulk liquid.

Key Outcomes from the Mesa Field Trial:

- Microalgae were cultivated on raw biogas for ≥ 7 weeks using MC. For the first 2 weeks of cultivation, the carbon transfer efficiency was ≥ 93%, and the carbon utilization efficiency was ≥ 71%. Although the CUE did not reach the target value of 80%, it appears to have been lowered due to the development of a complex ecological community in the liquid and on the biofilm. On the one hand, the MC membranes accumulated biofilm that was not suspended and, therefore, not harvestable. On the other hand, the communities had diverse heterotrophic bacteria that oxidized organic matter and provided an alternative source of CO_2 to the microalgae. Furthermore, predators and insects consumed microalgal biomass and also generated CO_2.

- The methane purity exiting the membrane lumen varied over the course of the project, from 80% around 10 AM to 3 PM and greater than 85% in the mornings and late afternoons, when photosynthesis was strongest. The largest limitation to achieving the targeted CH_4 purity of ≥ 97% was the counter diffusion of O_2 into the membrane, although out-diffusion of CH_4 also played a role. Future research is needed to identify better membranes that can deliver CO_2 more selectively.
- Methane-oxidizing bacteria and their functional genes were identified in the bulk-liquid and biofilm samples; phylotypes most similar to these bacteria dominated the genus abundance, particularly in the biofilm. The strong abundances of phylotypes of CH_4-oxidizing bacteria and methane-oxidizing genes support the hypothesis that CH_4 transferred across the membrane wall was oxidized, which significantly reduced its escape to the atmosphere.

Task 8 – 25-m^2 MC/Raceway setup and cultivation at AzCATI and data analysis

Due to supply chain restrictions and vendor delays, AzCATI developed and built custom 25-m^2 raceways (**Figure 8.1**). However, due to the delays, the ponds were not completed until the end of July 2021. *Scenedesmus obliquus* UTEX 393 was selected for cultivation as the seasonal organism that tolerates low salinity. Due to bacterial contamination, cultivation trials were limited to less than 1 week in duration but provided valuable time to validate functionality prior to installation at the Northwest Water Reclamation Plant. Because of the short trial performance, Milestone 8.2.1 utilized data from the onsite trials with raw biogas in task 7.

Figure 8.1. Installation and setup of 25-m^2 raceways on the westside of the AzCATI field site at ASU. Note that raceways were designed and built by the staff and students of AzCATI.

Key Outcomes: Custom 25-m^2 raceways were built and outfitted with temperature monitoring and pH control. These raceways were built and designed by the staff and students of AzCATI. The raceways were tested for leaks, paddlewheel mixing, and sensor logistics prior to transfer to the City of Mesa Northwest Water Reclamation Plant.

Task 9 – Techno-Economic Analysis (TEA)

The Techno-Economics team worked alongside the experimental and modeling teams to estimate the economic costs and benefits of the Membrane Carbonation (MC) process. The key assumption of this project's TEA was that we would study the TEA of the MC unit process only. While it is important to understand the costs of algal cultivation, the required assets and operational expenses, excluding carbon dioxide delivery and consumption, are not materially alterred by this project's achievements.

Cost Model for CO_2 Delivery and Transfer to Growth Medium

The Preliminary Techno-Economic Model was improved upon to integrate a wide variety of experimental results under several conditions. Previous TEA models linked together a powerful finite element mass transport model which allowed for analysis of a wide range of gas compositions, operating pressures, and constricted volumetric flow.

The analysis presented in this document is based on the detailed experimental results from growth trials. The cost model incorporates mass transfer results (CO_2 flux, CO_2 loss, and methane leakage) as a function of inlet pressure in the fiber bundles. In keeping with previous efforts by this team, we calculate the levelized cost of carbonation (LCOC) using the following financial and operational variables in **Equation 9.1**:

$$LCOC\left(\frac{\$}{MT(CO_2)}\right) = \frac{Installed\ Membrane\ Costs(\$) + \sum_{n=1}^{N} \frac{Operating\ Costs(\$)}{(1+r)^n}}{\sum_{n=1}^{N} \frac{a\, j_0\, (1-D)^n}{(1+r)^n}}$$

Equation 9.1. Levelized Cost of Carbonation

where:
N = Lifetime of the Membrane (years)
r = discount rate (% per year)
a = area of installed membrane (m^2)
j_0 = mass flux of CO2 before degradation (MT/year-m^2)
D = degradation rate of the membrane (% per year)

Estimating the installed membrane costs has consistently been one of the largest challenges in this project. Over the course of our research, we have talked with academic and industry experts, secured quotes of analogous products from vendors, and found vendor quotes to public municipalities for analogous products. With the assistance of polymer experts, we constructed a detailed cost model for the production of hollow-fiber membranes (HFMs) based on geometric/material inputs. We also unsuccessfully attempted to find private sector contract manufactures of hollow fiber membranes. Manufacture of HFMs is a continuous process with very low material costs and very high "machine setup" costs. We estimate that a product using commodity polymers produced at large scale can be produced for prices less than \$2/m^2. We calculated the costs of the Mitsubishi Rayon membrane to be roughly \$0.21/m^2 in chemical and utility costs. The bulk of expenses in mature fiber membrane businesses are "soft costs" derived from engineering, research, management, and sales expenses. The operational expenses of the membrane carbonation apparatus are primarily contributed by electrical expenses to run the gas compressor. The compressor was assumed to operate at 63% efficiency of ideal compression based on analysis of vendor specification sheets at appropriate scales.

Pure CO_2 Delivery at nth Plant Scale

In order to meet ***Milestone 9.2.2***, we conducted an analysis of pure CO_2 delivery at Nth Plant Scale. This milestone sought to demonstrated that CO_2 could be delivered to the growth medium for ≤$59/tonne assuming a cost of $50/tonne-$CO_2$(g). Using experimental data from the project, we make the following assumptions and calculations (**Table 9.1**). In this table, we distinguish

Table 9.1. N[th] plant cost calculations for 100% CO_2 delivery in satisfaction of Milestone 9.2.2.

Membrane Assumptions			
Cost of CO_2 (Farm Gate)	$	50.0	$/MT
Cost of CO_2 (Distribution)	$	1.5	$/MT
Cost of CO_2	**$**	**51.5**	**$/MT**
Gross Membrane Flux		2,640	g / m^2 / d
Membrane Cost	$	15.0	$/$m^2$
Membrane Lifetime		10.00	years
Real Discount Rate		4.00%	
Carbon Transfer Efficiency		99%	
CO_2 Content- Inlet Gas Mixture		100%	
Membrane Calculations			
Membrane Calculations			
Membrane Flux - calendar day		1,100	g / m2 / d
Membrane Flux - yearly		0.402	MT / m2 / y
Lifetime Flux			
Lifetime CO_2 Delivered to solution (MT)		4.02	MT / m2
Levelized Cost Calculations (membrane + CO2 losses)			
Real Discount Rate		4.00%	
Levelized Cost / MT		$56.6	$/MT-CO2
Cost Contribution of the Membrane		**$5.1**	**$/MT**
Compression Costs			
Membrane Operating Pressure (gauge)		310	kPa
kWh to Compress 1 MT CO_2 in Mixture		21.6	kWh/MT
Compressor Efficiency		63%	
Total Energy Requirements		34.2	kWh/MT
Total Cost of Compression		**2.18**	**$/MT**
Total Cost of CO_2 to Solution		**$59**	**$/MT**
Total Cost of Membrane Unit Operation		**$7.3**	**$/MT**

between Gross CO_2 Flux (g/m^2/day) and actual Membrane Flux (g/m^2/calendar day) which accounts for the membrane being active for 10 hours per day (daylight hours). Depending on the configuration of the algal farm, we might deduct the costs of compression, as those costs might be allocated elsewhere. For example, if a CO_2 pipeline is contractually obligated to deliver high-

pressure CO_2, then it is nearly free to step the pressure down to our membrane's operating pressure and we would have no need for compression.

First Customer Analysis

While we believe that the MC process can be economical at scale, we also researched its potential to provide value for early adopters. We conducted an interview with Qualitas to understand their potential needs as a buyer of a membrane carbonation product. The following analysis is based on their qualitative input. They did not share proprietary cost information, but provided essential information to further commercial product design. The objective of the First Customer analysis is to demonstrate that membrane carbonation could provide cost savings in the form of lower CO_2 purchases at small scale. We used the assumptions listed in **Table 9.2** to derive the allowable cost of the membrane given a desired payback period. We assumed, based on cultivation experience and literature, that the garden soakers used for CO_2 sparging in shallow ponds will result in 50% CTE to the growth medium. We assumed that the potential customer is able to procure delivered CO_2 at a cost of $125/tonne, which may be much lower than actual market prices. For reference, ASU Gas Services and AzCATI procure delivered liquid CO_2 on a bulk contract from a large gas distributor for roughly $500/tonne. By calculating the CO_2 purchase savings, we determine that the allowable membrane cost for a first customer will be $172/m^2. Using our hollow-fiber membrane production cost model, we anticipate that we could produce the membranes for $50/m^2, assuming that we supported a customer base with total 1000 acres under cultivation. Such a manufacturing operation would require approximately $1.0 million in Capital Expenses (ignoring R&D, startup costs) for the spinning line and supporting equipment. It would employ approximately 8–10 full time equivalent employees, including engineers, operators, and clerks. By demonstrating that a customer could justify purchasing the MC product at a higher price than our "all-in" manufacturing cost, we believe that the product could be financially viable as a startup enterprise assuming a large enough customer base could be developed quickly.

Table 9.2. Assumptions for first customer analysis

Item	Value	Units	Source / Note
Total CO_2 Purchase	2500	tonnes/year	Customer Interview
CO_2 Flux	1100	g/m^2/calendar-day	Project Data
CTE	99%		Project Data
Soaker CTE	50%		Team Estimate
Cost of CO_2	$125	$/tonne	Team Estimate
Seasonality Factor	1.46		
Payback Period	5	Years	Customer Interview

Figure 9.1 shows the relationship between cost of CO_2 ($/MT), the customer's existing infrastructure CTE (e.g,. soaker hose), and the breakeven membrane cost ($/m^2). The yellow star indicates that we believe our first customer has a current CO_2 cost of $100/MT and current CTE of 50%, thereby resulting in a willingness to pay of $50/m^2 for a MC product.

Comparison of Traditional Biogas Separation (Skid Mount) to Membrane Carbonation

The final effort carried out by the team was to compare the costs and benefits of traditional biogas separation (membrane or pressure swing) versus the membrane carbonation process. We carried this detailed analysis with the help of staff at City of Mesa Arizona's Northwest Water Reclamation Plant and with a report drafted for them by Arcadis. We used cost data and vendor quotes to provide our estimate of what a biogas separation system / Membrane Carbonation process tandem could deliver to a co-located an algal cultivation facility.

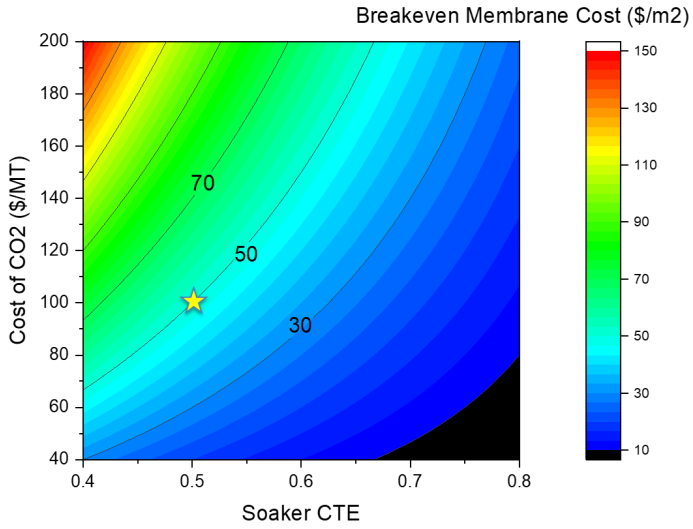

Figure 9.1 Iso-Cost Curve for First Customer Analysis.

"Business As Usual" Biogas Separation Followed by Membrane Carbonation

We first studied the "Business as Usual" Scenario 1, which was sized to NWRP's biogas availability. The process flow diagram for this concept is displayed in **Figure 9.2**. Sizing of equipment and energy requirements were conducted via a rigorous system simulation in Aspen

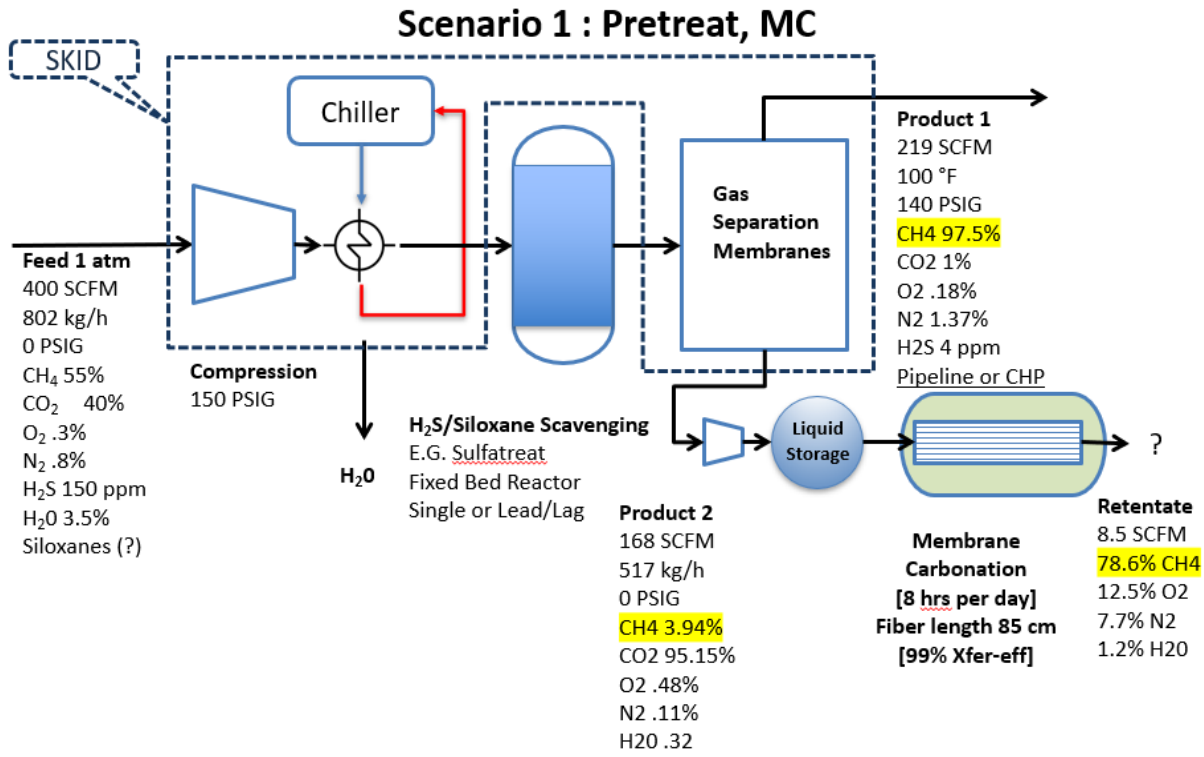

Figure 9.2. Process flow diagram for "business as usual" skid-based biogas separation, delivered to Membrane Carbonation.

Plus. Costs of equipment were sourced from Aspen Capital Cost Estimator and the Arcadis Report.

The economics are displayed in **Table 9.3**. The "Business As Usual" process takes "free" biogas (40% CO_2/55% CH_4/5% Other), and uses a Gas Separation Skid to separates it into two gas streams. The CO_2 is pressurized for liquid storage during non-growth hours. The CO_2 is then delivered to ponds via the MC process. The retentate from the MC process is a small amount of roughly 80% methane, an artifact from the non-perfect separation that occurs in the skid. We have not addressed what must be done with this methane. An algal cultivator co-located with the biogas facility could offset the cost of the separation capital and operational expenses through sales of the refined methane. We have assumed a credit of $4 per MCF for the methane. This analysis indicates the cost of the operation is greater than the revenue, and that the cost of CO_2 would be $50/tonne-$CO_2$.

Table 9.3. Economic evaluation: *in situ* Membrane Carbonation biogas separation

Captital Expense Calculation			**Annual Expense Calculation**		
Item	**Total Cost**				
Biogas Compressor	$	207,936	Loan Rate		5%
Biogas Cooler	$	25,000	Project Life		20
Retentate (RNG) Compressor	$	86,328	Capital Recovery Factor		8%
Retentate (RNG) Cooler	$	15,000	**Capital Charge**	**$**	**164,857**
Biogas Pressurized Storage	$	245,000			
Carbonation Membrane Bundles	$	409,745	Operating and Maintenance Costs	$	34,170
Condensate Return and Chiller Piping	$	20,000	Electricity	$	122,763
Digester Gas Piping and Fittings	$	35,000	H_2S/Siloxane Pretreatment Costs	$	178,704
Product Gas Piping and Fittings	$	20,000	**Total Operating Expenses**	**$**	**335,637**
RNG to Pipeline Metering Station	$	75,000			
Equipment Subtotal	$	1,139,009	**Total Yearly Expenses**	$	500,494
Electrical (10%) of Equipment Subtotal	$	170,851	Revenue Offset @ $4/MCF	$	461,594
Mechanical (10%) of Equipment Subtotal	$	113,901	**Net Expenses**	$	38,901
Installed Subtotal	$	1,423,761			
General Conditions (11% of Installed)	$	156,614			
Total Direct Installation Subtotal	$	1,580,375	**Cost per Tonne CO_2 delivered to MC**	**$**	**8.9**
Contingency (10%)	$	158,038			
Taxes, Insurance (5%)	$	79,019			
Overhead, Contractor (15%)	$	237,056			
Total Project Capital	**$**	**2,054,488**			

In Situ Biogas Separation via Membrane Carbonation

The second scenario studied involves separation via the membrane carbonation process. The process flow diagram for this concept is displayed in **Figure 9.3**. As studied, the membrane has the capability to selectively deliver CO_2 to the growth media while retaining methane. The proposed process flow diagram includes compression, water knockout, storage, siloxane/H_2S scavenging, membrane carbonation, and recompression for delivery to customer. The modeled product gas had a 93.6% methane content, which compares similarly to experimental results.

The economics of this process were examined in the same manner as in Scenario 1 (**Table 9.3**). Assumptions for the membrane carbonation cost and performance are the same, with the exception that CO_2 flux is assumed to decrease linearly with CO_2 partial pressure. Therefore, more membrane was required as the CO_2 content was assumed to be 41 %v/v. Again, biogas

sales offset the cost of operation. The cost of CO_2 as delivered to the ponds are determined to be \$9/tonne CO_2. We believe that process improvement, including more selective membranes, could allow the operator to receive renewable fuel credits (e.g., RINS) which would result in "free" CO_2 and a cashflow-positive operation. Currently, the retentate from the MC fibers does not meet pipeline standards. Better selectivity in the fibers could also allow improve this product marketability parameter.

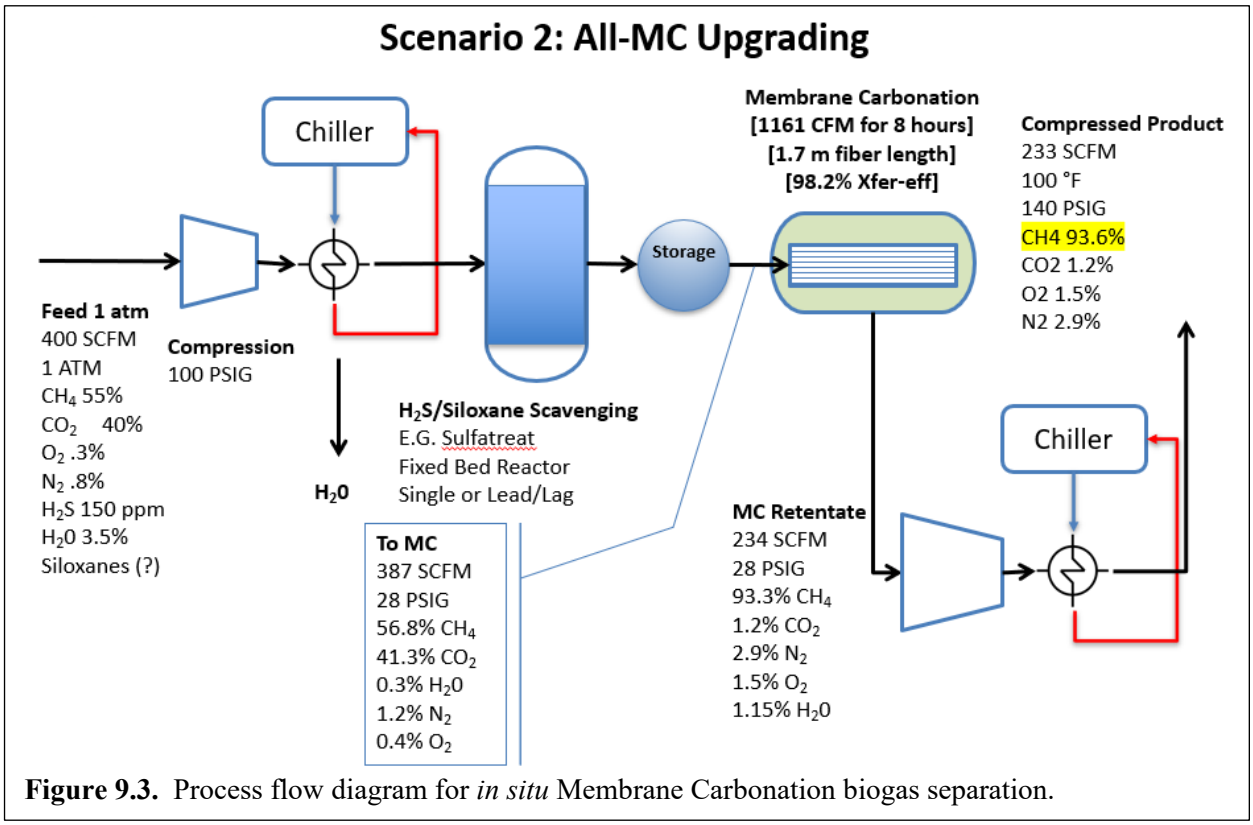

Figure 9.3. Process flow diagram for *in situ* Membrane Carbonation biogas separation.

Key Outcomes:

- Membrane Carbonation can deliver CO_2 for cultivation at a cost equal to or less than \$59/tonne, assuming CO_2 procurement at \$50/tonne. (***Milestone 9.2.2***)
- First Customer Analysis determined that membrane cultivation has quantitative cost savings and qualitative appeal for existing algal cultivators (e.g., Nutraceuticals). Assuming a payback period of 5 years, the cost to manufacture the device is significantly less than the customer's willingness-to-pay. Furthermore, customers expressed interest in reducing CO_2 emissions as caused by sparging inefficiencies ("Green Factor").
- Improving the CUE from 20% (baseline TechFin) to 80% results in an improvement from 9 g CO_2/g AFDW to 2.25 g CO_2/g AFDW. This results in a cost savings of \$338/MT-AFDW. If we assume an HTL fuel production process produces 125 GGE/tonne-biomass, then this results in a savings of \$2.7/GGE.

Task 10 – Life Cycle Assessment (LCA)

The LCA work is founded on understanding the greenhouse gas (GHG) emissions associate with the production of fuel from algae through a hydrothermal liquefaction (HTL) production pathway. The process flow diagram for the system is presented in **Figure 10.1**. The work leverages an engineering process model to accurately capture the energy and mass of the system. The outputs from the engineering process model are then coupled with life cycle inventory data to evaluate the environmental impact of the system through greenhouse gas (GHG) accounting. The end results of the life cycle assessment is directly compared to the renewable fuel standard. The report is divided into sections that detail the engineering process model and the life cycle assessment assumptions.

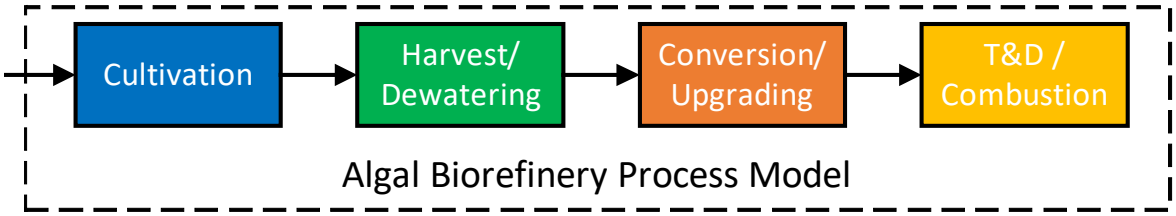

Figure 10.1. Process flow diagram and sub-unit process models developed for evaluating the system. The system boundary of the process is defined with the black line and is equivalent to a well to wheels.

Three scenarios are modeled: three different carbon-transfer efficiencies, carbon utilization efficiencies, and methane leak rates. A summary of the inputs for the three scenarios is presented in **Table 10.1**.

Table 10.1. Summary of the carbon efficiencies and methane leak rate for the three modeled scenarios.

	CTE	CUE	Methane Loss
Mitsubishi Rayon HFM	90%	65%	10%
Optimal HFM	95%	85%	1%
Biogas Skid	99%	90%	0.01%

Engineering process modeling

The engineering process model was developed to accurately capture the performance of the microalgae biorefining concept. The engineering process model include unit process operations for cultivation, harvesting, conversion, delivery, and combustion of the final fuel product. Major assumptions for each of the unit process operations are defined in the following sections. The model was developed to represent an *n*-th scale facility with hourly resolution.

Cultivation: The cultivation process was modeled based on an open raceway pond with carbon delivered through the developed MC system. The performance of the membrane system was based on the experimental work developed in this project. The assumption in the system was the biogas was delivered at pressure with a minimal pressure drop, specifically 5 psig. The biogas was assumed to be 40% CO_2 and 60% methane. The model includes the use of a dynamic growth model such that temporal variation was captured. To determine microalgal biomass

yields, this study adopted the biological modeling methodology developed by Greene et al.[15] This model calculates algae growth based on the primary physical processes affecting growth: culture temperature, respiration losses, and light availability as affected by culture concentration and incoming solar radiation. The model correlates a carbon-fixation rate to multiple efficiency factors that account for conditions deviating from optimal. Further details are presented in Greene et al. The annual average biomass productivity determined by the model was 23 g m^{-2} d^{-1}. The biomass concentration in the ponds over the course of one year is presented in **Figure 10.2**. The modeling of the biomass production with hourly time-scale enables understanding the carbon requirements on an hourly basis. The total energy consumption for the cultivation state if presented in **Figure 10.3**.

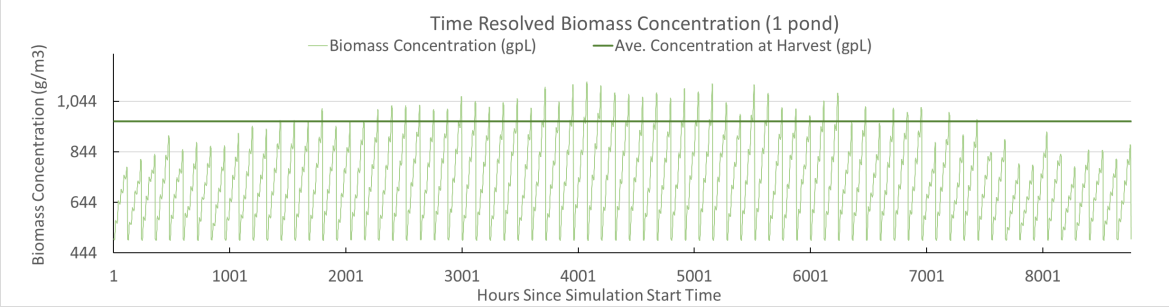

Figure 10.2. Modeling results illustrating the biomass concentration in the ponds.

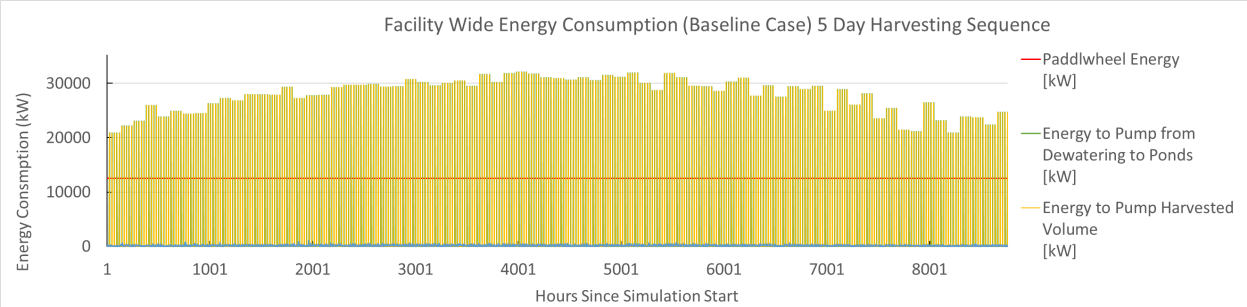

Figure 10.3. Summary of cultivation energy required for the operation of the facility.

Dewatering: The biomass dewatering process for the produced biomass consisted of three stages: a settler followed by a membrane and then a centrifuge. The settler was assumed to bring the biomass from 0.07% solids to 1% solids. The membrane achieved 13% solids, and finally the centrifuge brought the volume to 20% solids. The dewatering systems required 0.04 and 1.35 kWh per cubic meter of throughput for the three stages, respectively, equating to a combined 0.06 kWh per cubic meter of throughput of the first stage (the volume of throughput decreases significantly between each stage). The energy demands of the system for the baseline pathway are presented in **Figure 10.4**. As illustrated the centrifuge dominates the energy in the dewatering system. The other two unit process operations represented here are membrane (green) and centrate sterilization (pink).

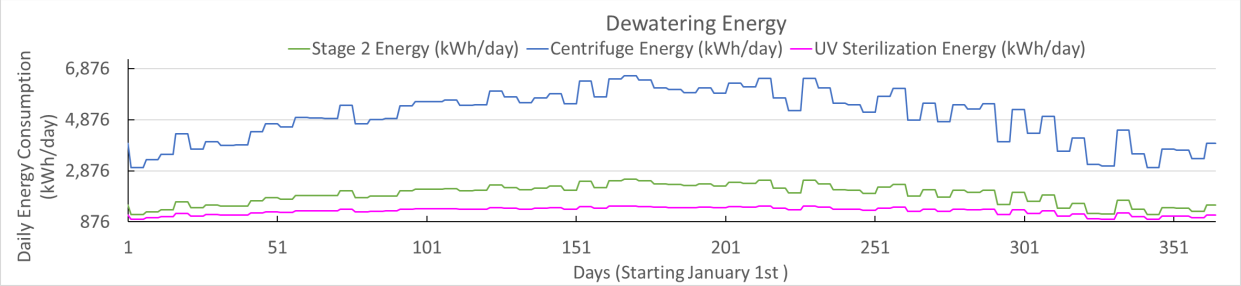

Figure 10.4. Dewatering energy demand over the course of 1 year using the described three stage dewater process. The three-stage dewatering system includes no energy input for the settling tank with the energy for the membrane (stage 2) and centrifuge presented. Additionally, the energy for media recycle is included and assumed to require UV sterilization.

HTL: The modeled system used HTL followed by hydro-treatment to convert the dewatered biomass to fuel products. The HTL and upgrading module were modeled closely after that of the Jones et al.[16] The dewatered biomass was pumped through a preheating system and then an HTL plug-flow reactor. The resulting products were divided by a filter and three-phase separator into char, aqueous material, and bio-crude. The bio-crude continued to a hydro-treating and hydrocracking process, where it was pumped through a series of columns and a heater to separate the crude oil into naphtha, diesel, and off-gasses. Meanwhile, the solid char was sold for the price of removal from the facility. The aqueous material was cooled and returned to the ponds for the purpose of recycling nutrients. This is assumed to be a seamless integration without any negative impacts in the growth system. The naphtha and diesel were taken to be stored and the off-gasses were processed in an ammonia scrubber.

The input flow rate to the HTL system was approximately 17 kg of dewatered biomass per second, although this would vary based on the productivity of the pond. The volume of fuels produced from HTL is governed by bio-crude yield, which ranged from 30% to 60%, with an average of 40%. The modeling work assumed a conversion efficiency of 41%. The model includes hydrocracking and hydrotreating to upgrade the biocrude to Diesel and Naphtha.

Transportation and Combustion: The final unit process operation is the distribution and final combustion of the fuel. This work assumed a pump to wheel emissions of 67.5 g $CO_{2\text{-eq}}$ MJ^{-1}.

Life Cycle Assessment Methodology

The outputs from the engineering process model are combined with life cycle inventory data to determine the greenhouse gas emissions of the system. Life-cycle inventory data were collected from the EcoInvent database using OpenLCA. GHG accounting includes three primary gases, CO_2, CH_4, and N_2O. The IPCC 100-year equivalency factors of 1, 28, 298, for the three gases were used, respectively. The results are thus presented in a carbon dioxide equivalence ($CO_{2\text{-eq}}$). The carbon accounting of the system includes the carbon uptake during growth as the assumption is the CO_2 supplied would eventually be atmospheric carbon. Thus, the combustion emissions are included in the carbon accounting.

Results

Three different scenarios were evaluated using the carbon efficiencies and methane leak rates presented in **Table 10.1**. The three scenarios are labeled, Mitsubishi Rayon HFM, Optimal HFM, and Biogas Skid. Each are more progressive in terms of improved performance. The results are compared to the renewable fuel standard (RFS) which represents a 50% reduction in emissions compared to conventional diesel which has a total emission of 92 g $CO_{2\text{-eq}}$ MJ^{-1}. Thus, the system must have a total emissions of less than 45 g $CO_{2\text{-eq}}$ MJ^{-1} to meet the renewable fuel standard.

Mitsubishi Rayon HFM: The LCA results for this scenario are presented in **Figure 10.5**. The results for the Mitsubishi Rayon HFM scenario are dominated by the significant methane loss associated with the system. This system assumes a methane loss rate of 10%. Because methane is a greenhouse gas that is 28 times worse than that of CO_2, the methane leak rate was detrimental to the environmental impact of the system. The total GHG emissions were 950 g $CO_{2\text{-eq}}$ MJ^{-1}. The methane leak rate accounted for 88% of the total positive GHG emissions in this scenario.

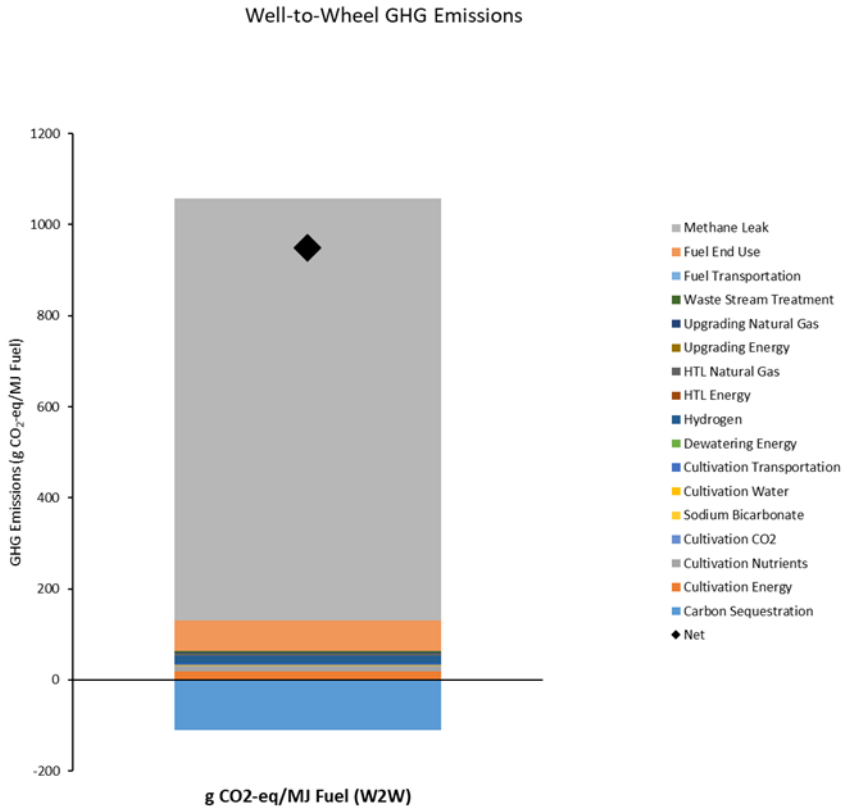

Figure 10.5. LCA results for the Mitsubishi Rayon HFM scenario. The net is presented with the black diamond.

Optimal HFM: The LCA results for the Optimal HFM system are presented in **Figure 10.6**. The total GHG emissions for this scenario are 88 g $CO_{2\text{-eq}}$ MJ^{-1}, which represents a dramatic (~ 12-fold) improvement over the Mitsubishi Rayon HFM scenario. The methane loss rate was reduced to 1% in this scenario, giving more than a one order of magnitude reduction in total emissions. The methane loss in this scenario accounts for 23% of the positive emissions and is

similar to the fuel use. This scenario does much better than conventional diesel, but still fails to meet the renewable fuel standard.

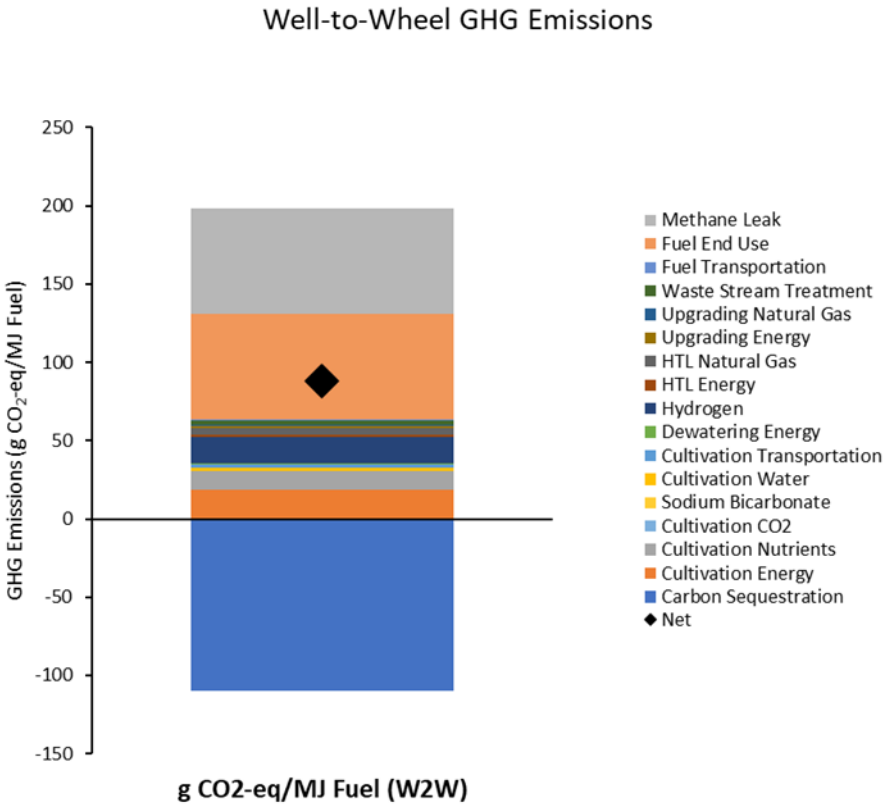

Figure 10. 6. LCA results for the Optimal HFM scenario. The net is presented with the black diamond.

Biogas Skid: The LCA results for the Biogas Skid scenario are presented in **Figure 10.7**. The total GHG emissions in the Biogas Skid scenario are 22 g $CO_{2\text{-eq}}$ MJ^{-1}, which meets the renewable fuel standard due to the dramatic reduction in methane loss, to less than 0.01%. The methane leak represents 0.05% of the total positive emissions from the scenario. Results from this scenario are more typical of traditional algal-based biofuel systems, with the results dominated by the carbon update, fuel use, cultivation energy, and conversion hydrogen.

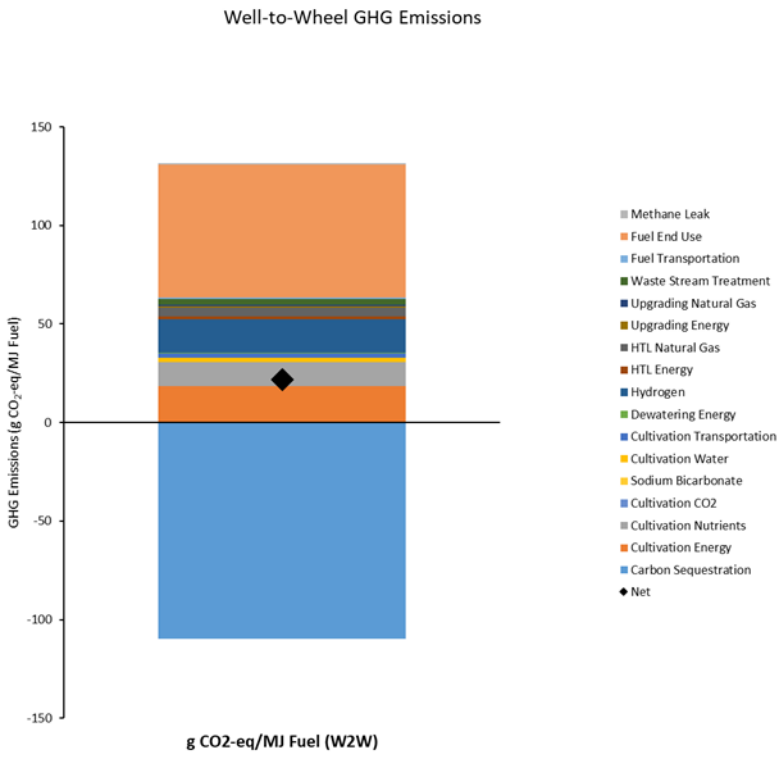

Figure 10.7. LCA results for the Biogas Skid scenario. The net is presented with the black diamond.

The total GHG emissions for the three scenarios are presented in **Table 10.2**.

Table 10.2. Tabulated LCA results for the three scenarios evaluated. Results are presented in units of g-CO_2-e MJ-1

	Mitsubishi Rayon HFM	Optimal HFM	Biogas Skid
Carbon Sequestration	-109.6	-109.6	-109.6
Cultivation Energy	18.4	18.4	18.4
Cultivation Nutrients	12.3	12.3	12.3
Cultivation Water	2.2	2.2	2.2
Cultivation Transportation	2.1	2.1	2.1
Dewatering Energy	0.4	0.4	0.4
Hydrogen	16.9	16.9	16.9
HTL Energy	1.3	1.3	1.3
HTL Natural Gas	4.6	4.6	4.6
Upgrading Energy	0.8	0.8	0.8
Upgrading Natural Gas	0.9	0.9	0.9
Waste Stream Treatment	2.7	2.7	2.7
Fuel Transportation	0.9	0.9	0.9
Fuel End Use	67.5	67.5	67.5
Methane Leak	927.2	67.2	0.6
Net	948.4	88.4	21.9

Key Outcomes:
The results clearly show that the methane-loss rate is critical to ensure the sustainability of the system in term of GHG emissions. The MC membranes must be robust to avoid and have high selectivity for the transfer of CO_2 over CH_4. A loss of more than 1% results in GHG results that cannot not meet the renewable fuel standard.

Products Developed

Technologies/Techniques

Prototype systems were developed for:

1. Membrane carbonation, consisting of hollow fiber membrane bundles arranged in sheets to deliver CO_2 from industrial waste streams as described in this report. Prototypes were 1 to 1.5 m^2 in surface area for the 4-m^2 raceways and 3 m^2 for the 25-m^2 raceways.

Invention/patent applications

1. **Methods and Systems for Membrane Carbonation**; Everett Eustance, Bruce Rittmann, Yen-Jung Lai, Justin Flory, Tarun Shesh, Diana Calvo; Provisional application filed in Mar. 5, 2019; Non-provisional application filed Mar. 4, 2020. No. 16/809,384. DOE notification on Dec. 12, 2018. Report No. 0488301-18-0068. DOE S-150,802 https://patents.google.com/patent/US20200283716A1/en

Publications

1. Lai, Y. S.; Eustance, E.; Shesh, T.; Frias, Z.; Rittmann, B. E. Achieving Superior Carbon Transfer Efficiency and PH Control Using Membrane Carbonation with a Wide Range of CO2 Contents for the Coccolithophore *Emiliania Huxleyi. Sci. Total Environ.* **2022**, *822*, 153592. https://doi.org/https://doi.org/10.1016/j.scitotenv.2022.153592.
2. Lai YS, Eustance E, Shesh T, Rittmann BE (2020) Enhanced carbon-transfer and -utilization efficiencies achieved using membrane carbonation with gas sources having a range of CO2 concentrations. Algal Research (52) https://doi.org/10.1016/j.algal.2020.102098
3. Eustance E, Lai YS, Shesh T, Rittmann BE (2020) Improved CO_2 utilization efficiency using membrane carbonation in outdoor raceways. Algal Research (51) https://doi.org/10.1016/j.algal.2020.102070

Manuscripts in Preparation

1. Eustance, E; Lai, Y. S.; Frias, Z; Potts, J; Forrester, J; Young, M; McGowen, J,.; Rittmann, B. E. Upgrading Biogas through Low Pressure Algal Membrane Carbonation. (In preparation for Energy and Environmental Sciences, Dec 2023)
2. Lai, Y. S.; Eustance, E.; Frias, Z; Michelle Young, M; Krajmalnik-Brown, R.; Rittmann, B. E. Methane upgraded along with membrane carbonation. (in preparation for Environmental Science and Technology, Dec 2023)
3. Eustance, E; Lai, Y. S.; Frias, Z; Potts, J; Forrester, J; Young, M; McGowen, J,.; Rittmann, B. E. Effects of Dilute CO2 in Flue Gas on the Performance of Membrane Carbonation. (In preparation for algal research, Dec 2023)
4. Lai, Y. S.; Eustance, E; Frias, Z;, Kalfus, R.; Young, M. Krajmalnik-Brown, R.; Rittmann, B. E. Microbial communities affecting methane upgraded along with membrane carbonation. (in preparation for ACS Sustainable Chemistry & Engineering, Dec 2023)

Presentations

1. Bruce Rittmann, "Microbial Photobioenergy: Making CO_2 a Resource, Not a Liability." New Jersey Institute of Technology Algae Workshop, Newark, NJ. Oct. 11, 2022
2. Bruce Rittmann, "Microbial Photobioenergy: Making CO_2 a Resource, Not a Liability." Zhejiang University, Hangzhou, China, virtual seminar. Aug. 19, 2022
3. Lai YS, Eustance E, Frias Z, Rittmann BE. A bleed- and venting-valve strategy enables membrane carbonation to achieve superior carbon transfer efficiency with industrial gas streams. Algal Biomass Summit, Virtual Conference, Sept. 28- Oct 27, 2021.
4. Eustance E, Lai YS, Flory J, McGowen J, Rittmann, BE. Utilizing Membrane Carbonation with Synthetic Flue Gas and Biogas in Outdoor Raceways. Presentation at Algae Biomass Summit, Sept. 9-11, 2020, Virtual.
5. Rittmann, B. E. (2020). Highly Efficient CO_2 Delivery from Industrial Sources. Presentation at the Algae Biomas Summit 2020 (August 20, 2022).
6. Bruce Rittmann, "Opportunities in Microbial Bioenergy" Guest lecture in FSE 150, Grand Challenges class taught by Prof. Haolin Zhu at Arizona State University, Tempe, AZ. Nov. 12, 2019
7. Bruce Rittmann, "Optimizing Microalgae Production by Delivering Sources of Concentrated CO_2" IWA Microalgae Conference, Vallodolid, Spain. July 2, 2019
8. Bruce Rittmann, "Optimizing Microalgae Production by Delivering Sources of Concentrated CO_2" Gordon Research Conference on Photosynthesis, Newry, ME
9. Bruce Rittmann, "Membrane Carbonation for 100% Efficient Delivery of CO_2 from Industrial Gases" (poster) Dept. of Energy BETO Conference, Denver, CO. March 7, 2019. Dr. Rittmann gave a poster presentation outlining the concept for the current proposal. The poster is not publicly available, but listed in the program (p. 11): https://www.energy.gov/sites/prod/files/2019/03/f60/BETOPeerReview-Program2019%20%28003%29_0.pdf
10. Bruce Rittmann, "Atmospheric CO_2 Capture, Enrichment, and Delivery" (talk) Dept. of Energy BETO Conference, Denver, CO. March 7, 2019. Dr. Rittmann gave a verbal presentation describing the MC technology when coupled with atmospheric CO_2 capture in the ACED project. https://www.energy.gov/sites/prod/files/2019/03/f61/Atmospheric%20CO2%20Capture%20and%20Membrane%20Delivery%20%28ACED%29_EE0007093.pdf

Media

1. Melina Walling, Arizona Republic, Algae could help fuel the future. But it's not easy being 'green', May 19, 2022 https://www.azcentral.com/story/news/local/arizona-science/2022/05/19/algae-could-fuel-planes-ships-and-cars-but-challenges-remain/6914853001/
2. Bailey Miller, Fox 10, ASU and Mesa team up for pilot project to remove greenhouse gases with algae, Feb. 10, 2022 https://www.fox10phoenix.com/video/1033538
3. Cameron Polom, ABC15: Algae could be key to reducing carbon emission in wastewater treatment process, Dec. 9, 2021 https://www.abc15.com/weather/impact-earth/algae-could-be-key-to-reducing-carbon-emission-in-wastewater-treatment-process
    a. Video clip: https://www.youtube.com/watch?app=desktop&v=apBCn2_wnmk
4. Elise Lange, ASU News: ASU researchers see potential in wastewater, Nov. 30, 2021 https://news.asu.edu/20211129-solutions-zero-waste-water

5. ASU News: ASU again among nation's top research universities, January 3, 2022 https://news.asu.edu/20220103-arizona-impact-asu-again-among-nations-top-research-universities
6. Arizona State University, "DOE awards $4.5 million to ASU teams to discover new ways to harness carbon dioxide for reducing cost of biofuel" ASU Now. Nov 7, 2018. https://asunow.asu.edu/20181107-discoveries-doe-awards-45-million-asu-teams-discover-new-ways-harness-carbon-dioxide/. This was the ASU press release from the initial DOE award announcement.
   Arizona State University, "ASU teams find new ways to harness CO_2 to reduce biofuel costs" Biomass Magazine. Nov 9, 2018. http://biomassmagazine.com/articles/15741/asu-teams-find-new-ways-to-harness-co2-to-reduce-biofuel-costs. The ASU press release was also published in Biomass Magazine.

Bibliography

1. Lai, Y. J. S., Eustance, E., Shesh, T. & Rittmann, B. E. Enhanced carbon-transfer and -utilization efficiencies achieved using membrane carbonation with gas sources having a range of CO2 concentrations. *Algal Res.* **52,** 102098 (2020).
2. Shesh, T., Eustance, E., Lai, Y. J. & Rittmann, B. E. Characterization of CO2 flux through hollow-fiber membranes using pH modeling. *J. Memb. Sci.* **592,** 117389 (2019).
3. Kim, H. W., Cheng, J. & Rittmann, B. E. Direct membrane-carbonation photobioreactor producing photoautotrophic biomass via carbon dioxide transfer and nutrient removal. *Bioresour. Technol.* **204,** 32–37 (2016).
4. Poehlein, A., Freese, H., Daniel, R. & Simeonova, D. D. Genome sequence of Shinella sp. strain DD12, isolated from homogenized guts of starved Daphnia magna. *Stand. Genomic Sci.* **11,** 1–8 (2016).
5. Kalyuzhnaya, M. G., De Marco, P., Bowerman, S., Pacheco, C. C., Lara, J. C., Lidstrom, M. E. & Chistoserdova, L. Methyloversatilis universalis gen. nov., sp. nov., a novel taxon within the Betaproteobacteria represented by three methylotrophic isolates. *Int. J. Syst. Evol. Microbiol.* **56,** 2517–2522 (2006).
6. Xu, X., Zhu, J., Thies, J. E. & Wu, W. Methanol-linked synergy between aerobic methanotrophs and denitrifiers enhanced nitrate removal efficiency in a membrane biofilm reactor under a low O2:CH4 ratio. *Water Res.* **174,** 115595 (2020).
7. Gutierrez, T., Whitman, W. B., Huntemann, M., Copeland, A., Chen, A., Kyrpides, N., Markowitz, V., Pillay, M., Ivanova, N., Mikhailova, N., Ovchinnikova, G., Andersen, E., Pati, A., Stamatis, D., Reddy, T. B. K., Ngan, C. Y., Chovatia, M., Daum, C., Shapiro, N., Cantor, M. N. & Woyke, T. Genome Sequence of Arenibacter algicola Strain TG409, a Hydrocarbon-Degrading Bacterium Associated with Marine Eukaryotic Phytoplankton. *Genome Announc.* **4,** 765–781 (2016).
8. Bowman, J. P. & Nichols, D. S. Aequorivita gen. nov., a member of the family Flavobacteriaceae isolated from terrestrial and marine Antarctic habitats. *Int. J. Syst. Evol. Microbiol.* **52,** 1533–1541 (2002).
9. Kersters, K., De Vos, P., Gillis, M., Swings, J., Vandamme, P. & Stackebrandt, E. Introduction to the Proteobacteria. *The Prokaryotes* 3–37 (2006). doi:10.1007/0-387-30745-1_1
10. Hoefman, S., Heylen, K. & De Vos, P. Methylomonas lenta sp. nov., a methanotroph isolated from manure and a denitrification tank. *Int. J. Syst. Evol. Microbiol.* **64,** 1210–1217 (2014).
11. Murrell, J. C. Molecular genetics of methane oxidation. *Biodegrad. 1994 53* **5,** 145–159 (1994).
12. McDonald, I. R. & Murrell, J. C. The particulate methane monooxygenase gene pmoA and its use as a functional gene probe for methanotrophs. *FEMS Microbiol. Lett.* **156,** 205–210 (1997).
13. May, T., Polag, D., Keppler, F., Greule, M., Müller, L. & König, H. Methane oxidation in industrial biogas plants-Insights in a novel methanotrophic environment evidenced by pmoA gene analyses and stable isotope labelling studies. *J. Biotechnol.* **270,** 77–84 (2018).
14. Hua, Z. S., Wang, Y. L., Evans, P. N., Qu, Y. N., Goh, K. M., Rao, Y. Z., Qi, Y. L., Li, Y. X., Huang, M. J., Jiao, J. Y., Chen, Y. T., Mao, Y. P., Shu, W. S., Hozzein, W., Hedlund,

B. P., Tyson, G. W., Zhang, T. & Li, W. J. Insights into the ecological roles and evolution of methyl-coenzyme M reductase-containing hot spring Archaea. *Nat. Commun. 2019 101* **10,** 1–11 (2019).

15. Greene, J. M., Quiroz, D., Compton, S., Lammers, P. J. & Quinn, J. C. A validated thermal and biological model for predicting algal productivity in large scale outdoor cultivation systems. *Algal Res.* **54,** 102224 (2021).
16. Jones, S. B., Zhu, Y., Anderson, D. B., Hallen, R. T., Elliott, D. C., Schmidt, A. J., Albrecht, K. O., Hart, T. R., Butcher, M. G., Drennan, C., Snowden-Swan, L. J., Davis, R. & Kinchin, C. Process Design and Economics for the Conversion of Algal Biomass to Hydrocarbons: Whole Algae Hydrothermal Liquefaction and Upgrading. (2014). doi:10.2172/1126336